

4D Printing: Enabling Technology for Microrobotics Applications

Georges Adam, Amine Benouhiba, Kanty Rabenorosoa, Cédric Clévy,
and David J. Cappelleri*

This review demonstrates that 4D printing constitutes a key technology to enable significant advances in microrobotics. Unlike traditional microfabrication techniques, 4D printing provides higher versatility, more sophisticated designs, and a wide range of sensing and actuation possibilities, opening wide new avenues for the next generation of microrobots. It brings disruptive solutions in terms of variety of stimuli, workspaces, motion complexities, response time, function execution, and genuinely 3D microrobots. This review brings to light how soft and smart materials directly printed in 3D are particularly well suited for microrobotics requirements. This review gives an overview of 4D printing in microrobotics, highlighting advanced microrobotics requirements, fabrication methods, used smart materials, activation techniques, recent advances in the microrobotics field, and emerging opportunities.

aerospace,^[8] automotive,^[9] aviation,^[10,11] consumer products,^[12] healthcare,^[13–15] construction,^[16] food,^[17,18] and education.^[19] Commonly used techniques for 3D printing include stereolithography (SLA), digital light processing (DLP), fused deposition modeling (FDM), multi-jet fusion (MJF), selective laser sintering (SLS),^[20,21] and direct metal laser sintering (DMLS),^[22,23] as well as other direct writing methods.^[24]

With the advent of the development of new materials capable of not only being 3D printed but also changing their structural shape and/or properties after being printed, a new field of 4D printing has emerged.^[25–27] While traditional 3D printing often leads to the creation of static solid

objects, 4D printing offers the created objects a dynamic behavior, manifested in adaptive, shape-shifting abilities, and/or material properties changes. Such abilities are enabled through the use of smart materials,^[28] such as shape memory polymers (SMPs), liquid crystal elastomers (LCEs), and hydrogels, among others. This dynamic behavior is activated by an external energy input, such as temperature,^[29] light,^[30] pH,^[31,32] and voltage,^[33] among other environmental stimuli. Furthermore, compared with traditional subtractive manufacturing, which is carried out by continuously removing material from a solid block, such as computer numerical control (CNC) machining, additive manufacturing offers many advantages,^[34] including fast prototyping/production, accessibility, cost-effectiveness, reduced material consumption, and almost unlimited geometric complexity in designs.


In addition to the endless possibilities of shapes that 3D/4D printing can offer, it also provides a broad spectrum of sizes. These sizes range from large macroscale objects, such as 3D printed buildings,^[35] to very small objects, such as micro- and nanodevices.^[36] One of the targeted applications for the latter devices is microrobotics. Unlike regular robotics, which relies heavily on DC/AC motors for actuation and a high number of assembled parts, microrobotics is typically based on materials with less complex, straightforward (mostly monolithic) designs. Consequently, 4D printing at a small scale holds very high potential in the field of microrobotics.^[37,38] Traditional microfabrication techniques (cleanroom technology) are highly limited in terms of design, geometries (mainly 2D shapes), and materials selection. By contrast, 4D printing introduces a new level of versatility and complexity into the forms and configurations

1. Introduction

Over the past two decades, 3D printing, also known as additive manufacturing, has been of great interest to scientists and engineers. 3D printing offers tremendous benefits as reduced cost in manufacturing, just-in-time production, improving human health, living up to environmental sustainability, and many others. It is the process of making 3D solid objects from a digital file.^[1,2] The solid objects can be made using a variety of different materials,^[3] including polymers, metals,^[4,5] ceramics,^[6] and composites.^[7] As a result, 3D printing can be found in numerous industries and has a wide range of applications, such as in

G. Adam, Prof. D. J. Cappelleri
Multi-Scale Robotics and Automation Lab (MSRAL)
Purdue University
205 Gates Rd., West Lafayette, IN 47906, USA
E-mail: dcappell@purdue.edu

Dr. A. Benouhiba, Prof. K. Rabenorosoa, Prof. C. Clévy
FEMTO-ST Institute
AS2M Department
University Bourgogne Franche-Comté, CNRS
24 rue Alain Savary, Besançon 25000, France

 The ORCID identification number(s) for the author(s) of this article can be found under <https://doi.org/10.1002/aisy.202000216>.

© 2021 The Authors. Advanced Intelligent Systems published by Wiley-VCH GmbH. This is an open access article under the terms of the Creative Commons Attribution License, which permits use, distribution and reproduction in any medium, provided the original work is properly cited.

DOI: 10.1002/aisy.202000216

produced on such a scale; it also allows for a simpler use and integration of a wide variety of smart materials. This renders the design of microrobots with more sophisticated geometries and advanced capabilities, a fast and cost-effective process. That said, this kind of technology comes with its own set of limitations and challenges, including structural control in time and space domains simultaneously, repeatability, printing resolution, printing speed, low viscous behavior, and so on.

The main objective of this article is to study the different promising technologies of 4D printing and their potential in the field of microrobotics. It provides a summary of the state of the art, as well as comprehensive outlines for the use of such technologies in microrobotics applications. Specifically, Section 2 addresses the motivation for 4D printing in microrobotics. Section 3 introduces different microfabrication methods and how they are modified to obtain 4D printing technologies. Section 4 presents different smart materials for 4D printing. Section 5 discusses the current state of 4D printed microrobotics, while the last section provides a future outlook into the next generation of 4D printed-enabled microrobots.

2. Motivation for 4D Printing in Microrobotics

2.1. Microrobotics State of the Art

Microrobotics has made considerable progress in the past 30 years. As an emerging field of research arising from the fusion of micro/nanotechnology and traditional robotics, it has stimulated the interest of the scientific community and opened new doors for a variety of applications. The latter includes micro/nanomanipulation, benchtop micromanufacturing, drug delivery, precision surgery, medical diagnosis, personalized medicine, and detoxification.^[39] Some examples of microrobotics applications are shown in **Table 1** where manufacturing and biomedical applications are separated and classified through the scale of manipulated objects.

Although microrobots experience the same forces as regular robots, these forces' magnitude is usually size-related and can vary with scale. At the microscale, the surface area-to-volume ratio increases considerably, thus rendering volume-related forces, such as inertia, gravity, and buoyancy, less relevant, and gives surface-related forces such as surface forces, fluid drag, and friction a dominant role.^[40] Such a trend is very apparent in nature (small insects). For example, small insects (water striders) use surface tension rather than buoyancy to stand on the water surface.^[41] Others can jump very high in relation to their size.^[42] Therefore, these particular physical phenomena must be taken into account when designing microrobots, whether when using traditional techniques such as cleanroom technology or advanced technologies such as 4D printing. For a more comprehensive analysis of such forces, the reader should refer to the study by Wautelet.^[43]

During the past decade, biomedical applications have become the primary targeted field for microrobotics,^[44] due to their small size, low weight, high flexibility, large thrust-to-weight ratio, and high sensitivity. In biomedical applications, small-scale robots must be biocompatible^[45] but are expected to work under different environments consequently with different sets of

Table 1. Several key microrobotics examples in manufacturing and biomedical applications versus the size of the objects being manipulated.

Size of objects		
Being manipulated	Manufacturing applications	Biomedical applications
Millimeter scale	Microoptical bench fabrication ^[83]	Ocular microsurgery ^[195]
Hundreds of micrometer	Microcoil assembly ^[196]	Ferromagnetic soft catheters ^[46]
	Fiber characterization ^[56]	Assisted in vitro fertilization ^[55]
Tens of micrometer	3D photonic crystal assembly ^[85]	Oocyte characterization ^[54]
–	–	Microstent fabrication ^[38]
A few micrometer	Nanotool mounting on an	DNA characterization ^[197]
–	Atomic force microscope cantilever ^[198]	Intracellular characterization ^[57]
–	Microhouse fabrication	–
–	On an optical fiber ^[86]	–

requirements. For example, in vivo and in vitro microrobotics (for lab-on-a-chip applications) do not have the same requirements. From hundreds of micrometer to the millimeter scale, in vivo microrobotic applications (see Table 1) include navigation through blood vessels by a ferromagnetic soft catheter,^[46] magnetic catheters,^[47] flagellated magnetotactic bacteria for localized drug delivery,^[48–52] and magnetic microrobots for eye microsurgery.^[53] In these applications, the requirements include miniaturized parts, constrained spaces, delicate/sensitive surrounding tissues, complex and precise operations, smart materials for actuation, sensing, and interfacing with the human body. For in vitro applications, oocyte mechanical characterization has been extensively studied^[54] along with spermot-assisted fertilization.^[55] The challenges here are how to maintain the position of the oocyte and to control the applied force to determine their stiffness. For manipulating objects smaller than 10 μm, two representative applications are DNA characterization using microtweezers^[56] fabricated by microelectromechanical systems (MEMS) technology, and intracellular characterization using magnetic microbeads and advanced biomedical imaging systems.^[57] Leong et al.^[58] presented origami-based tetherless microgrippers. Among other functionalities, these microgrippers can be used for the capture and retrieval of objects and conducting biopsies. The microgrippers were fabricated using standard cleanroom/microfabrication technology. A magnetic field was utilized to guide the grippers in vivo to their desired target remotely. Also, once they reached the target, a locking mechanism can be activated either by heat (40–60 °C) or by using a variety of different chemicals, including organic chemicals.

In diagnosis and health monitoring, microrobotics has also shown great promise. Fischer et al.^[59] presented a smart dust biosensor for remote sensing. The hybrid microdevice is powered by adenosine triphosphate (ATP) and relies on antibody functionalized microtubules and kinesin motors to transport the target analyte into a detection region. Bassik et al.^[60] expanded on the previous work by specializing in the activation mechanism of the microgrippers. A biopolymer with a selective enzymatic degradation was utilized in the hinges of the

microgrippers. The biopolymer will naturally degrade in cancerous environments, which will then trigger the closing mechanism of the microgripper. In the field of dentistry, microrobots can find diverse applications, including major tooth repair, cavity preparation and restoration, orthodontic treatment, diagnosis and treatment of oral cancer, improving tooth durability and appearance, and many other applications.^[61]

Other microdevices that can improve disease diagnostics are lab-on-chip devices.^[62,63] They can improve diagnostic speed, cost efficiency, sensitivity, and ergonomics. From a robotic point of view, the developments are focused on actuation, sensing, and control. Various actuation strategies have been investigated, such as dielectrophoresis (DEP),^[64–70] magnetophoresis,^[71,72] electro-wetting on a dielectric (EWOD),^[73] and surface acoustic wave (SAW) activation.^[74] For sensing, exteroceptive sensors are typically used for proof-of-concept.^[63] Indeed, proprioceptive sensors are challenging to integrate in the lab-on-chip devices.^[64,75,76] Brazey et al.^[77] proposed an impedance-based real-time position sensor to monitor and control cell displacements during their motion in the chip. The variation of the impedance inside the chip, measured between two electrodes and induced by the passage of the cells, is used to obtain their positions. For more details on cell manipulation technique comparisons, one can refer to the study by Ghallab and Badawy.^[76]

Despite the benefits and high potential for microrobotics for healthcare applications, some disadvantages and potential hazards do exist.^[78] For example, certain metallic coatings such as nickel, mainly used in microrobot designs for its magnetic capacities, are known to be allergenic, carcinogenic, toxic, and teratogenic in certain forms and/or in high doses.^[79] The presence of high amounts of silver used, in some cases, for the fabrication of hinges in multisegment nanorods, can cause discoloration of the skin and internal organs. However, no negative health effects have been noted for silver.^[80] Foreign DNA, usually used in some microrobot designs for its biocompatibility as a natural biopolymer, can result in immunologic and inflammatory responses.^[81] In addition, high levels of UV light, which are sometimes utilized as an input control signal for microrobots, are known to cause skin damage and, in worst cases, skin cancer (depending on the delivered laser power). Furthermore, other hazardous situations can arise due to poor navigation and task execution. For instance, loss of navigation control and the targeting of an erroneous site leading to healthy cells' damage are considered to be worse than failing to accomplish the desired task. Nevertheless, there are some efforts aimed at limiting these risks, to name one, the work of Iacovacci et al.^[82] on the retrieval of nanoagents from the bloodstream.

Microrobotics can be classified according to two approaches: tethered and untethered. Tethered microrobotics has been the first historical approach investigated and was initially aiming at miniaturizing robots and systems. Tethered robotic systems embed their own actuation, tool (typically used for manipulation or for characterization), and also quite often one or more sensors. The tether of the robot enables energy to be delivered to the system and the ability to collect sensing data in a variety of modalities. Tethered microrobots can apply large forces and bring a tool with dexterous manipulation and sensing capabilities in contact with an object/component to be studied or manipulated. Many commercial microrobotic systems today are tethered systems and

this approach has widespread manufacturing applications. A few examples include the fabrication of a microoptical bench,^[83,84] 3D photonic crystal^[85] (see Table 1), lab-on-fiber devices,^[86] and the fabrication of other microstructures^[87] as well as being used for the characterization of many kinds of objects and components.^[88,89] Recently, key works have been achieved to calibrate commercially available tethered robotic systems, demonstrating that complex motions can be done with high position accuracy (better than 100 nm).^[90–92] Physical-based modeling and robust control have also been successfully implemented on tetethered microrobotic systems, demonstrating their potential to guarantee the performance of these robotic systems despite strong environment changes.^[93,94] To further improve capabilities, research on integrated sensors that are able to provide high-quality measurement close to the point of contact between robot and object it is interacting with has also been pursued.^[95–97] In addition, novel actuation principles based on smart materials and associated kinematic designs are being investigated. For instance, Haouas et al. proposed a parallel kinematic robot with seven degrees-of-freedom (DoF) with dexterous grasping capabilities.^[98] A millimeter-scale tethered microrobot, inspired by the art of kirigami and assembled via a pop-up process, that utilizes a piezoelectric actuator, was constructed into a delta robot configuration to achieve high-bandwidth and high-precision operations.^[99] Finally, methods for the optimal design and/or control-oriented design methods of compliant mechanisms with embedded actuation are being studied for performance improvement and a higher density of functions for similar or smaller design footprints.^[100]

Untethered microrobotics appeared after tethered microrobotics and brought with it a more disruptive approach in its principles. Contrary to tethered microrobotics, untethered systems generally do not embed their own actuators. The untethered microrobot is a microscale object that is moved or deformed by external force fields. These external force fields can take many forms, such as magnetic,^[101–104] light,^[105,106] acoustic,^[107–112] etc. These mobile microrobots, ranging in size from a few tens of micrometers to few millimeters, allow them to be used in very small environments and enable very good mobility at high speeds. For these reasons, untethered microrobotics today has been very widely developed. As shown in **Figure 1**, four types of stimuli are typically used to achieve remote actuation of microrobots. The most developed stimulus is magnetic actuation which has been used to demonstrate planar and 3D positioning, multirobot actuation, and complex task execution (see **Figure 1**).^[113–120] Some micromanipulation techniques not shown in **Figure 1** are the following: optical trapping that can achieve 2D^[121–124] and 3D^[125,126] manipulation, as well as multiple objects manipulation.^[127–129] Second, the generation and manipulation of microbubbles by means of temperature gradients induced by low power laser radiation was introduced by the study of Farahi et al.^[130] and then improved in the study by Ortega-Mendoza and co-workers.^[131,132] More recently, micromanipulation based on laser-induced thermocapillary convective flows at the fluid/gas interface was demonstrated for single^[133] and multiple objects.^[134] To compare and understand the advantages and disadvantages of magnetic and optical actuation for microrobotics, we invite the reader to refer to the study by Sitti and Wiersma.^[135]

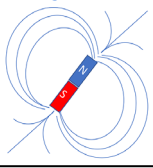
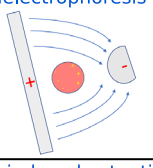

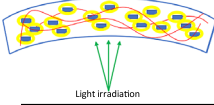

Stimulus	2D	3D	Multi-robots	Complex tasks
 Magnetic	Pawashe et al. [101] Jing et al. [102] Barbot et al. [103] Dkhil et al. [104]	Martel et al. [48] Barbot et al. [113] Oulmas et al. [114] Hu et al. [49] Wu et al. [50] Leclerc et al. [51] Jing et al. [52]	Diller et al. [117] Chowdhury et al. [118] Pawashe et al. [115] Mahoney et al. [119] Tottori et al. [120]	Salehizadeh et al. [116]
 Dielectrophoresis	Miled et al. [64] Kharbout et al. [65] Michalek et al. [66] Xu et al. [67] Subramanian et al. [68]	Iliescu et al. [69] Chu et al. [70] Huang et al. [176]	 <p>Trend to the next microrobotics generation</p>	
 Light induced actuation	Jia et al. [105] Palagi et al. [106]	Martella et al. [170] Zeng et al. [171]		
 Acoustic	Qiu et al. [107] Matouš et al. [108]	Guo et al. [109] Ozcelik et al. [110] Tao et al. [111] Ren et al. [112]		

Figure 1. State of the art of untethered microrobotics systems for micromanipulation, microassembly, and complex tasks.

Microrobotics has achieved substantial advances in the last few years.^[136] In fact, advanced fabrication technologies have enabled microrobotics to take important steps. Cleanroom fabrication techniques (standard lithography, etching, etc.) have enabled the first steps of microrobotics. It was followed by 3D printing through two-photon lithography commercialized by Nanoscribe in 2007. The rapid development of soft and smart materials which can be printed in 3D with high resolution is expected to open a new age for next-generation advanced microrobotics. The requirements for such systems are described next.

2.2. Advanced Microrobotics Requirements

There are a wide range of requirements necessary to achieve advanced microrobotic functions that are not currently available from commercially available systems. They are shown in **Table 2** and described in the following section.

Despite the wide and diverse scope of applications and interests, critical to achieving them is the need for microrobotic systems to have integrated tools adapted for the particular task at hand. Regarding scaling issues, it is of primary interest that these tools consider the dominance of surface forces, and more widely, the specifics of the contact occurring between the object or component of interest and this tool. Indeed, these contacts are strongly dependent not only on both the object/component itself but also on the environment (temperature, hydrometry, charges, etc.). Thus, achieving robotized tasks efficiently at the microscale requires the simultaneous consideration of the robot, its tool, the working environment, and the object/component that is being studied/manipulated. This is because of the strong coupling of their behaviors, which is contrary to case in macroscale robotics. This intricate coupling is a key paradigm for several reasons.

Table 2. Summary of key microrobotic requirements.

Integrated functionalities	Tools (end-effectors) with sensor(s)
Overall size of the microrobot	<1 mm ³
Minimum number of DoFs	3
Repeatability of the microrobot	<100 mm
Dynamic control speed	kHz range

First, the lack of knowledge about the behavior and physical phenomenon happening at the microscale are not well known, and thus predicting their behavior has only been established for some very specific cases. As a result, the need to integrate sensors that can measure the dynamic changes in physical quantities (position, displacement, force, pH, temperature, current, etc.) very close to the point of contact and/or in the environment is of utmost importance. This challenge is more significant in the usual actuator and sensor integration issues because they are fully taking part in, then influencing, the robot in the working environment. The principle chosen must then clearly tend to limit (or make it known) the influence of sensors and actuators to the behavior of the whole robotic system. In this scope, multimodal sensing is a noticeable trend. Therefore, the first advanced microrobotics requirement is the capability to actuate/control microrobotic systems with tools that can efficiently and dynamically act and sense the robot/environment interactions.

The second key requirement for the next-generation microrobotic systems lies in the size of the instrumented robot. Indeed, smaller sizes would open up many wider applications by making it possible to investigate smaller environments (i.e., in vivo and in vitro), improving the robot dynamics, and improving their precision. Despite the wide scope of applications and needs,

microrobotic instrumented systems having a size smaller than 1 mm^3 is a key but realistic challenge.

The third key advanced microrobotics requirement is related to the mobility and/or dexterity of the next-generation microrobotic systems. Mobility in a typical 3D workspace of a few hundreds of micrometers along each axis is needed in most applications. Also, the capability to move around the object/component of interest in the workspace is of key interest. Thus, microrobotic systems having at least three DoFs are ideally required to enable sufficient dexterity/mobility in space.

Most microrobotic systems are intended to be used for characterization and manipulation purposes. In this scope, users strongly expect not only repeatable but also accurate behavior to assess performances in a statistical way. The need to study influential parameters notably appears as a key need for both scientific and industrial investigations. The repeatability of a robotic system appears directly dependent on the physical principle used to generate the motions, while its accuracy can be largely improved using modeling and calibration approaches. Nevertheless, improving the accuracy is only feasible for repeatable robots. Thus, the next key advanced microrobotic requirement is for the microrobotic systems to have repeatability on the order of 100 nm. This level of repeatability is directly dependant on the microrobot materials and fabrication process used to create the microrobots. For instance, purely elastic behaviors and compliant or continuous based motion transformation principles allow for increased repeatability.

The last key advanced microrobotics requirement is related to the control of the next-generation microrobotic systems, which can be used to achieve many critical tasks. The control of motions, trajectories, and the interactions between a robot and its environment/object in a dynamic way are of key interest. Control directly enables the worker to use the robot as it is required and expected. Two emerging aspects are of typical interest. The first one lies in the dynamics. Indeed, the next-generation microrobotic systems will be much smaller and much more instrumented than they are today. This will result in the system having drastically higher dynamics with bandwidths higher than 1 kHz becoming feasible, enabling the achievement of tasks at high frequencies. The expected limitations of such systems are not known today and will clearly constitute key new challenges as well. The second key requirement in regard to control is related to the end users (biologists, mechanical engineering, chemists, etc.) of the next-generation microrobotic systems. These users will need to use the systems without having advanced knowledge in control engineering and robotics. In this aspect, a key challenge will be to develop control algorithms that can self-adapt and reconfigure to the tasks and to the environment but that also enable intuitive use through ergonomic human-machine interface.^[137]

Making the transition from macro- to microrobotics comes with many advantages, but it also gives rise to many challenges. Scaling down notably modifies what are the main influential phenomena inducing strong modification of choices to be done at the microscale compared with the macroscale. Microrobotic systems can thus be made from many different/emerging materials, inorganic materials, such as polymers (elastomers, gels, liquid crystals), metals (mainly but not exclusively noble metals), ceramics (piezoelectric materials), composites, and/or organic

materials, such as the case for biohybrid microrobots, where living components (living cells or organisms) are added to chemically provide power for motion and other tasks.^[138] Some of these materials have enabled the 3D printing of microstructures. This new approach can help lift the traditional limitations inherent with 2D-based cleanroom fabrication technology.

In terms of actuation, microrobotics can benefit soft actuators based on smart materials able to achieve large deformation, complex/programmable motions, and produce enough forces or torques for the application requirements. Furthermore, with regard to sensing, the amplitudes of the physical aspects to be sensed associated with such a scale are usually in the range of uncertainties and noise for full-scale sensing systems. Also, finding lightweight power solutions for macro robots is already a highly challenging task, and it becomes much more problematic for microrobotics, as options for micro- and nano-batteries are very limited.^[138] Consequently, many alternative solutions, strategies, and novel methods are being investigated and explored for material selection, design, fabrication, actuation sensing, and power of micro- and nanorobotics. One of the highly promising technologies for all these challenges is 4D printing.

3. 4D Printing at Small Scales

In the past few decades, with the boom of the microchip and transistors industries, microfabrication techniques have been steadily improving with the goal of minimizing the structures and improving resolution. However, the fabrication processes are still the most limiting factor for the development of microrobotics, especially due to the inherit 2D nature of most used microfabrication techniques. Currently, the most common microfabrication technique consists of classic lithography, in which a photosensitive material is exposed to UV light of a certain wavelength with the use of a mask and a light source. With the exposure of the photoresist material to light, it undergoes a chemical reaction that changes the solubility of the photosensitive material. For positive photoresist, the exposed area increases the solubility, and for negative photoresist, it decreases. After immersion in a developer solution, the high-solubility region would be removed, thus creating the desired pattern on the substrate.

This is a very reliable and well-studied method since it has been around for so many years, and the minimum resolution keeps improving. The most common methods of reducing the resolution consist of using lower wavelength light or using a different medium for light propagation (immersion lithography systems). However, as lithography is an optical method that requires a mask, the resolution will ultimately be limited by the diffraction limit, which sets the minimum distinguishable distance between two features before light interference acts on the substrate side of the mask. The diffraction limit (d) is given as the quotient of the wavelength (λ) by a factor of the medium's index of refraction (n) and the half-angle subtended by the objective lens (θ) or numerical aperture (NA) of the optical system, as shown in Equation (1).

$$d = \frac{\lambda}{2n \sin(\theta)} = \frac{\lambda}{2nNA} \quad (1)$$

One method to improve the resolution is to increase the index of refraction of the medium. Instead of light traveling through air

($n = 1$), immersion lithography systems are used so that the liquid's index of refraction is greater ($n > 1$). Current state-of-the-art lithography systems use a ArF excimer laser with working wavelength of 193 nm.^[139] Table 2 shows the best resolution of an optical lithography system given a working wavelength 193 nm and the diffraction limit for both dry and immersion systems. Most commercially available systems can only reach a resolution of ≈ 500 nm because it becomes exponentially more expensive to reach the diffraction limit.

Another method that poses a solution to the diffraction limitations of optical systems is called e-beam lithography (EBL), in which a tightly focused beam of electrons is used to pattern a structure in specific photosensitive materials. This is a type of maskless lithography because no mask is required and the electron beam is able to trace out the desired pattern on the substrate. This method can achieve resolutions in the sub-10 nm range,^[140–142] as shown in Table 2. However, one major limitation of these two lithography methods is the ability to fabricate complex 3D structures. These methods create patterns layer-by-layer, and it is possible to create undercuts and simple 3D with sacrificial layers or etching methods, but it becomes expensive and the ability to create complex 3D structures is still limited. Some works have demonstrated the ability of fabricating a flat structure using photolithography methods that subsequently curls up into a 3D shape after fabrication; however, these structures are still limited in terms of geometries and ease of fabrication/prototyping. For example, Huang et al.^[143] developed a hydrogel microrobot that is fabricated using a bilayer structure and photolithography, which curls up into a helical shape after the fabrication process is complete.

A more versatile and common fabrication method consists of 3D printing; however, the resolution is not as fine. The most common printing methods are FDM and SLA. FDM melts the material and uses a nozzle to build the desired structure, while SLA uses a photochemical process to selectively cross-link photosensitive material, creating a structure. Both methods allow the fabrication of complex 3D shapes; however, the resolution is not comparable to that of lithography techniques. Another relatively new method that combines some advantages of stereolithography and standard lithography methods is called projection microstereolithography ($P_{\mu}SL$). This method creates a virtual photomask with a projector and polymerizes the material layer-by-layer, which is changed by the use of a motion stage to move the material sample.^[144] Table 3 shows the best resolution for current FDM and SLA printers, but most available systems have a much poorer resolutions. It also shows the resolution of $P_{\mu}SL$.

Recently, with the development of high repetition-rate laser systems, two-photon polymerization (TPP) has become a highly sought after method because it combines the versatility of 3D printing with the resolution of lithography techniques.^[145,146] Indeed, Figure 2 shows the future manufacturing methods are trending to complex 4D geometries with low nanometer-level resolutions, enabled by this technique. TPP uses the principle of two-photon absorption, which states that an atom can absorb two or more photons simultaneously, thus allowing the electrons to transition to states that were not possible with single-photon absorption. This process is governed by a virtual transition state that has extremely short duration (in the order of femtoseconds);

Table 3. Comparison of different fabrication methods, including standard microfabrication and 3D printing methods, as well as new technologies that enable more flexible microfabrication.

Method		Best resolution	Complex 3D/4D geometry	Ref.
Optical lithography	Air/dry	107 nm ^{a)}	No	[139]
–	Immersion	74 nm ^{a)}	No	[139]
EBL		2 nm	No	[140,141]
Standard 3D printing	FDM	20 μm ^{b)}	Yes	[199]
–	SLA	25 μm ^{b)}	Yes	[200]
Projection microstereolithography	$P_{\mu}SL$	3 μm	Yes	[144]
Micro 3D printing	TPP	70–100 nm	Yes	[145,146,201]

^{a)}These values are the best possible resolution based on the diffraction limit, assuming a state-of-the-art ArF excimer laser source,^[202] which has a wavelength of 193 nm. Most commercially available systems can only reach around 500 nm resolution; ^{b)}These values refer to the vertical resolution of the best FDM and SLA printers. The smaller nozzle size for FDM printers is around 250 μm and the laser spot for SLA printers around 140 μm , so the feature sizes cannot be printed in the low-micron range reliably. An industrial SLA printer can have tolerances around 30 μm .

thus, the lasers need to be fast enough to excite this virtual state. This is a nonlinear process and the polymerized cross-sectional area scales with the inverse square of the laser intensity, so the laser beam can enter the photoresist and only trigger polymerization in a small region around the focus point. Outside of this small volume, the probability of two-photon absorption is extremely rare, resulting in increased resolution. As shown in Figure 3B, this polymerization method allows for a tight polymerization region, only on the focused region of the laser. When compared with traditional photopolymerization (Figure 3A), the polymerized region is much larger, resulting in lower resolution.

For TPP, the laser radiation interacts with a photosensitive material, creating a highly localized chemical reaction that polymerizes the substrate, creating the desired structure. The entire TPP process consists of three separate processes: 1) initiation, in which the photoinitiators reach the excited state due to two-photon absorption and decompose to radicals, 2) propagation, where the radicals combine with monomers, and 3) termination, where monomer radicals are combined creating long cross-linked chains and terminating the polymerization process. In other words, the two-photon absorption triggers photodissociation (breaking of C–C bonds in the photoinitiator), creating highly reactive radicals that will bond with monomers, starting the radical polymerization process. This process ends when a radical reacts with another. In most cases, the photoresist material formulation will have a photoinitiator, which is simply a material with a low photodissociation energy, thus increasing the overall material's photosensitivity. This entire process, combined with the tight focus of the high power/high repetition-rate laser, allows the fabrication of complex 3D structures with very high resolution, currently around 100 nm, as shown in Table 2.

As a comparison, SLA uses a UV laser to induce photopolymerization through single-photon absorption on the surface of

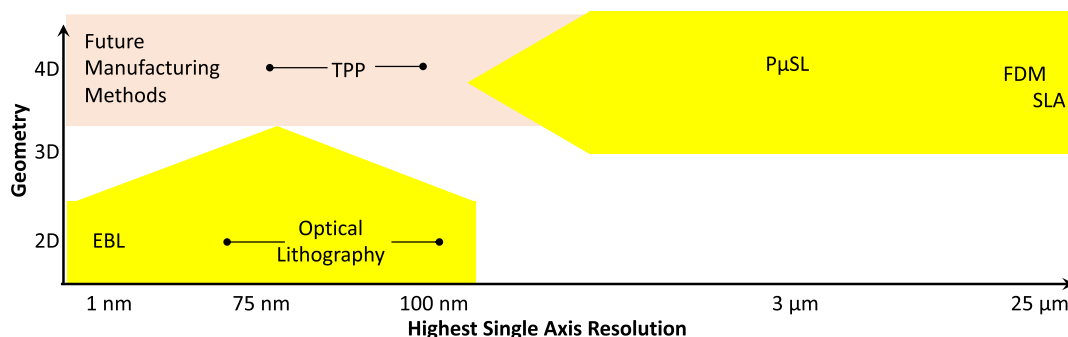


Figure 2. Plot of geometric dimension capability versus highest single axis resolution for the small-scale fabrication methods shown in Table 4. Future manufacturing methods are trending to complex 4D geometries with low nanometer-level resolutions.

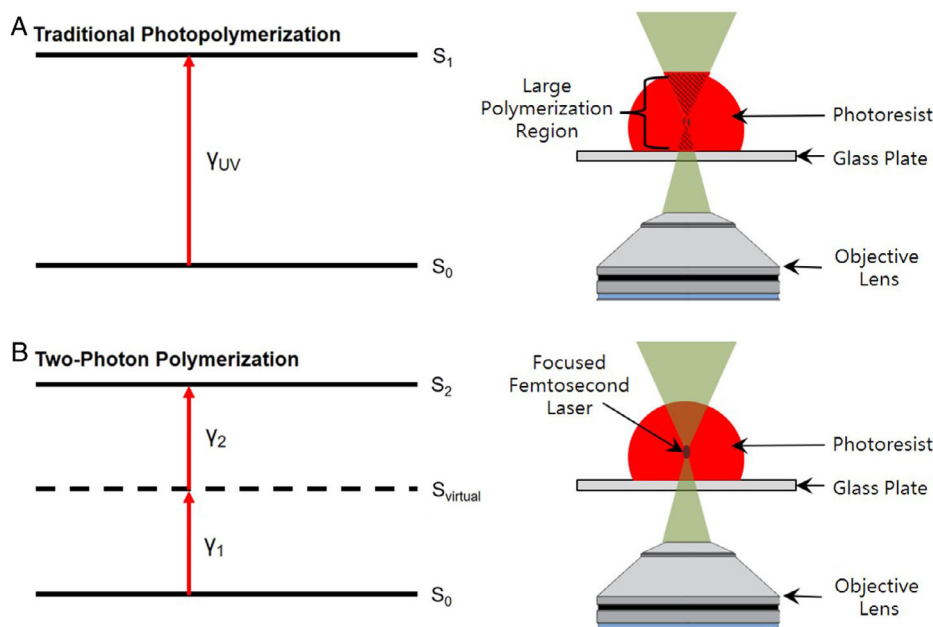


Figure 3. Schematic comparing traditional photopolymerization using UV light with TPP in the IR range with a femtosecond laser. A) With the absorption of the UV photons (γ_{UV}), the electrons move to a higher energy state (S_1), polymerizing the entire shaded region. B) The two-photon absorption reaches an even higher electron state (S_2) via the virtual state ($S_{virtual}$), resulting in polymerization of only the focused region.

the material, thus only being able to fabricate structures using a layer-by-layer approach. In contrast, as most photoresist materials are near transparent in the infrared (IR) range and highly absorbent in the UV range, TPP can be initialized with fast IR laser pulses focused on a small volume of material. Therefore, TPP can fabricate materials with complex 3D geometries, differently from the layer-by-layer approaches that other methods use.

Furthermore, there is a wide variety of materials that can be used for micro-3D printing, such as hydrogels or other organic compounds, which will be discussed further in Section 4. This provides a high degree of versatility because complex microstructures can be fabricated using functionalized materials, resulting in multi-DoF structures. Here, we will be focusing on 4D structures fabricated by TPP, in which the four dimensions consist of the three spatial dimensions plus time. In other words, 3D structures are able to change over time, as response to stimulus or

environment. This response includes change in size, color, or even complete degradation, among others.

4. 4D Printing Materials

One of the main advantages of TPP printing is its versatility and multi-DoF capabilities that its wide range of materials enable. There are two main types of materials used for TPP: single-phase materials and multiphase materials (or nanocomposites). Single-phase materials are completely miscible; however, their characteristics depend on the blend type and print settings, such as laser power and exposure time. The photoresist is activated by the high energy density laser which results in efficient cross-linking of the material. On the contrary, a nanocomposite is a multiphase material that relies on light-triggered cross-linking of organic and hybrid siloxane-organic photoresists. It uses fillers

that can be dispersed in a wide range of materials, often providing novel and remarkable properties while keeping its original structural integrity. Recently, a third type of material for TPP printing has been gaining traction: biomaterial-based compounds. These materials use widely studied biomaterials, such as some types of proteins, and create a composition that can be printed using TPP, giving it novel properties while being biocompatible, such as specific cell affinity.

4.1. Single-Phase Materials

One of the main attractive features of single-phase materials for TPP is that they have a great performance from a processability standpoint. Most issues encountered in the printing process are due to irregularities in the material which usually arises from immiscible particulates in the composites. However, this is not a problem here because the material is homogeneous. On the contrary, it is typically more difficult to achieve certain material properties when compared with a multiphase material, such as achieving magnetic and conductive properties. Next, different single-phase photoresist blends will be presented along with the properties they provide to the printed structure.

While TPP presents a suitable method for fabricating high-resolution multi-DoF microrobots, they are susceptible to shrinkage and collapse during the fabrication procedure. Therefore, it is highly desirable to develop methods to enhance the mechanical properties of the printed material. The easiest method is to optimize the fabrication settings, such as exposure time and laser power, effectively controlling the level of cross-linking. In addition, using a development approach with a UV radiation treatment has been shown to further cross-link the structure resulting in improved stability.^[147] Another method is to mix different materials that are more rigid into the blend, such as mixing polyvinylpyrrolidone (PVP)^[148] or exciting a preexisting polymer chain instead of simply the standard liquid monomer solution.^[149]

For microrobotic applications, the actuation potential of a material is of great importance, oftentimes even more than optical or mechanical properties. There have been many different single-phase material formulations that actively respond to external stimulation resulting in motion or change in volume. For these applications, the use of different hydrogels is extremely beneficial because, in general, they are made out of a network of hydrophilic polymeric chains, which are able to absorb large amounts of water and change volume. Hydrogels can be fabricated in such a way that they will respond to external stimuli, thus creating a smart material. Furthermore, the ability to actively control the swelling of a microrobot is especially beneficial for biomedical applications because it can be used as a mechanism to trigger the release of a drug payload or to biodegrade the microrobot after its use, leaving no footprint behind.

Numerous studies have shown a wide variety of external stimuli that can cause swelling and shrinking of the TPP printed structure. These stimuli include changes in pH,^[148,150] changes in solvent environment,^[151,152] light,^[153] and temperature-controlled solvent intake/release,^[154] among others. Hu et al. have developed a bioinspired hydrogel structure that presents shape transformation due to changes in pH and is capable of trapping

microobjects. To increase the swelling ratio, the cross-linking density of the TPP process has to be relatively low, which can result in poor mechanical strength. However, PVP was added to the photoresist blend, increasing its viscosity and mechanical strength. In another study, Tudor et al. designed a hydrogel blend that is capable of high swelling ratios (around 300%) and can be fabricated with submicron resolution. In addition, the swelling ratio is temperature dependent, allowing volume changes only above a certain temperature threshold. The use of LCEs has also been investigated for TPP printing because these substances behave similarly to liquids, but they show a high degree of orientation along one particular (long) axis. Therefore, a polymer chain fabricated with an LCE results in highly oriented structure, causing swelling/shrinking in a preferred direction, displaying an anisotropic response.^[155] One of the downsides of using such stimuli for shrinking and swelling is that they are diffusion-based, so they are inherently limited in their response time. Design parameters can be optimized both in the geometry and in the material formulation to speed up the response time. For many microrobotic cases, this actuation method is to be used in drug delivery applications, in which speed of release does not play a crucial role.

In addition to the tremendous versatility and great resolution that TPP provides, one of the main factors for the success of this fabrication method in biomedical applications is the fact that many of the commercially available photoresists are inherently biocompatible. These materials include OrmoComp, IP-DIP, and poly(ethylene glycol) diacrylate (PEGDA). In most cases, using a commercially available photoresist provides great functionality and it has been studied more in-depth than custom blends, making it a great starting point. Nonetheless, some properties, such as magnetism, cannot be achieved using a single-phase material. One solution used by multiple studies is to coat the structure in a metallic layer postfabrication, giving it magnetic properties.^[156–158] Another approach is to use a multiphase material, as will be discussed further in Section 4.2.

Researchers have also developed novel biomaterial-based photoresist resins that can be used in the TPP process to fabricate biocompatible structures. The great advantages of using a biomaterial-based resin are that they will be biocompatible while retaining the structural integrity and mechanical properties of the polymer, and the cell affinity of the biomaterial. Several proteins have been used as base materials for TPP printing, such as bovine serum albumin (BSA). They have been deeply characterized, are low cost, and can provide different stimulus responses.^[159–161] Lastly, single-phase photoresist materials can provide a wide range of versatility and functionality, such as refractive index modulation and surface tunability (mainly used for metamaterial applications), surface functionalization (which is optimal in single-phase photoresists due to uniform distribution of functionalized groups), and for the fabrication of conductive structures.

4.2. Multiphase Materials

In general, multiphase materials for TPP can provide more functionality and additional DoF in an actuation and sensing point of view when compared with single-phase photoresist resins. Some

material properties are much more difficult to achieve with single-phase rather than multiphase materials, for instance, controllable magnetic properties. However, as mentioned before, a single-phase material will be easier to fabricate because there is only one phase to take into account when setting fabrication conditions. As an example, magnetic nanoparticles (NPs) floating in a photoresist resin can react with the laser radiation and locally heat up, causing bubbles and resulting in defects to the fabricated structure. Thus, material choice and concentrations must be taken into account carefully, as they greatly affect the final properties of the structure.

As in the case for homogeneous materials, enhancing the mechanical properties of the printed structure can, in turn, increase its complexity. One of the most common methods when using multiphase materials is to add single or multiwall carbon nanotubes (CNTs) to the photoresist mixture. During the fabrication, the CNTs can be aligned to the print direction and the mechanical properties enhancement can be tailored based on the length and diameter of the CNTs. Furthermore, CNTs have been shown to also have conductive properties, allowing the fabrication of specially tailored conductive polymers using TPP.^[162,163] There are other methods to fabricate a conductive polymeric structure using TPP, such as the use of a gold NPs precursor to create conductive channels^[164,165] or other metals.^[166] The main issue of using metals is that they have a high refractive index, which can interfere with the laser, resulting in poor resolution and even local heating of the resin that causes bubble formation.

For biomedical applications, such as cell stimulation and differentiation, the use of custom-made 3D structures with piezoelectric properties made possible by TPP is of great use. The differentiation of osteoblast cells has been demonstrated using a printed piezoelectric structure made out of OrmoComp (commercially available photoresist) and barium titanate NPs.^[167] TPP can also be used to print structures onto piezoelectric materials, which can use vibrations as an actuation method, as demonstrated in the study by Kim et al.^[168]

Another main consideration with TPP printed structures is the Young's modulus and mechanical stability of the printed structures. **Figure 4** shows a comparison between different materials commonly used in microfabrication, especially 3D/4D printing. As shown, the Young's modulus of hydrogel formulations is significantly lower than the one for commercially available photoresists. Therefore, many studies add materials such as PVP to increase the Young's modulus of the printed structure. In addition, laser power and exposure time can be set in a way to control the mechanical properties of TPP printed structures and even provide a pathway for actuation. Hippler et al.^[169] used poly(*N*-isopropylacrylamide) (PNIPAM) to fabricate a light-responsive bilayer cantilever. By controlling the exposure parameters during the printing process, they were able to control the cross-linking of the material, thus achieving different material properties from each side of the cantilever. This design showed highly attractive actuation properties, due to its high and entirely reversible deformations (maximum curvature deformation of $0.15 \mu\text{m}^{-1}$ for a cantilever length of $40 \mu\text{m}$), fast response time (within 100 ms), and versatile and robust fabrication process. In general, multiphase materials are interesting and promising but have issues with low-Young's modulus, which might be a limiting factor for microrobotic applications.

For many microrobotic applications, magnetic actuation is widely used due to its inherent benefits, such as wireless actuation, ease of integration, and ability to scale the systems. One of the main methods to add magnetic properties to a TPP printed structure is to disperse magnetic NPs in the desired photoresist, which still keeps the properties of the photoresist while adding magnetic capabilities. Combining magnetic particles with hydrogels previously mentioned can provide novel results, such as a remote controllable microrobot that is biocompatible and can use swelling properties to create on-demand drug delivery. **Table 4** and **5** show a number of different materials used to fabricate 4D printed microrobotic structures, their respective stimuli, and response associated with each.

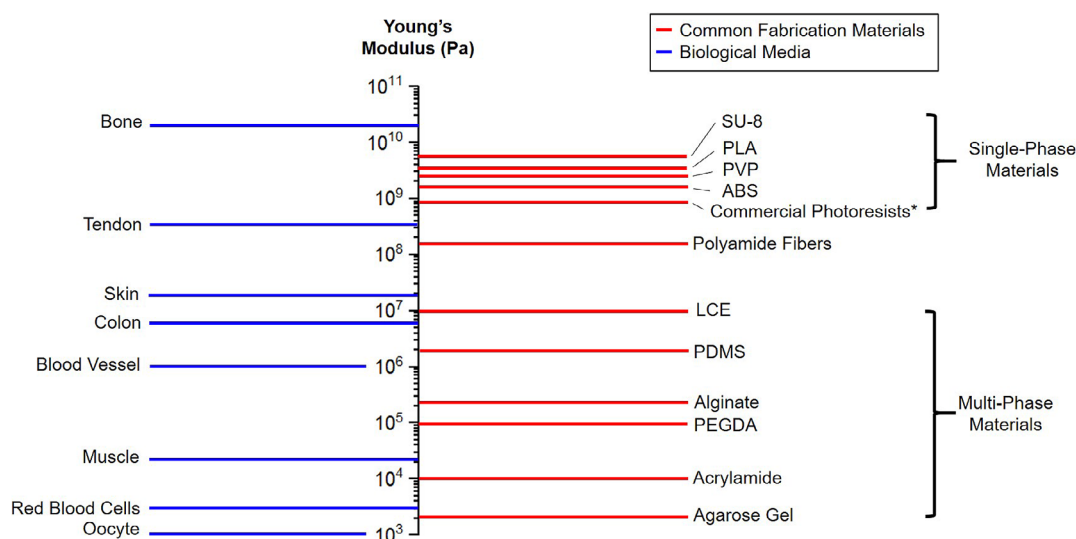


Figure 4. Young's modulus of different materials commonly used in microfabrication and 3D/4D printing,^[179–186] as well as different biological media.^[187–193] Note: these are approximate values and the TPP fabrication settings, such as writing density, laser power, and exposure time, can greatly influence the mechanical properties of the printed structures. *These include commercial photoresists such as IP-DIP, IP-S, and OrmoComp.

Table 4. Summary of 4D printed multi-DoF microrobots using TPP fabrication and showcasing stimulus responses and possible applications. The stimulus response/locomotion principle is corkscrew-like for all microrobot types listed unless mentioned in the notes column.

Material composition	Geometry	Size	Actuation input	Number of DoF	Robotic system	4D properties	Ref.
PEGDA + PETA + Fe ₃ O ₄	3D (rigid cylinders connected by compliant springs)	200 × 8 μm	Oscillating magnetic field (undulatory locomotion)	3 (1 translation + 2 rotations)	Untethered (hard)	Biodegradable (water cleaved in 12 h)/Drug delivery	[172] Figure 5A
PEGDA + PETA + Fe ₃ O ₄	3D (artificial bacterial flagella-helical)	28 × 3 μm	Rotating magnetic field	3 (3 rotations)	Untethered (hard)	Biodegradable (4 h)/Drug delivery	[203]
PEGDA + PETA + Fe ₃ O ₄ + 5-FU	3D (helical)	120 × 40 μm	Rotating magnetic field	3 (3 rotations)	Untethered (hard)	Drug delivery/Alternating magnetic field causes plasmonic heating for drug release and heat therapy/Biodegradable	[175] Figure 5D
Gelatin methacryloyl + P2CK (photoinitiator) + Fe ₃ O ₄ (added postprinting)	3D (helical)	30 × 3.5 μm	Rotating magnetic field	3 (3 rotations)	Untethered (soft)	Drug delivery via enzymatic degradation/Biodegradable	[204]
Gelatin methacryloyl + photoinitiator + Fe ₃ O ₄	3D (double helical)	20 × 6 μm	Rotating magnetic field	3 (3 rotations)	Untethered (soft)	Drug delivery via enzymatic (MMP-2) degradation/Biodegradable (5–118 h)	[173]
Methacrylamide chitosan + photoinitiator + SPIONs	3D (double helical)	20 × 6 μm	Rotating magnetic field	3 (3 rotations)	Untethered (soft)	Drug delivery via light induction/Biodegradable (204 h)	[174] Figure 5B
IP-DIP + Ni/Ti coating	3D (helical)	26 × 7 μm	Rotating magnetic field	3 (3 rotations)	Untethered (hard)	Able to attach and move immotile sperm cells/Drug delivery/Biocompatible	[55]
IP-DIP + Ni/Ge coating	3D (helical)	100 × 30 μm	Rotating magnetic field	3 (3 rotations)	Untethered (hard)	Structural color response/Drug delivery	[158]
SU-8 or IP-L + Ni/Ti coating	3D (helical)	8.8 × 2 μm	Rotating magnetic field	3 (3 rotations)	Untethered (hard)	Biocompatible, able to transport microparticle by caging mechanism/Drug delivery	[157] Figure 5E
SU-8 + Ni/Ti coating	3D (screw inside cylinder forming a syringe micromachine)	175 × 30 μm	Rotating magnetic field	3 (3 rotations)	Untethered (hard)	Drug delivery via micro-vortex and microsyringe mechanism	[176] Figure 5F
SU-8 + Fe ₃ O ₄ + HlgC + FITC	3D (helical, single twist-type, double twist-type)	60 × 9 μm	Rotating magnetic field	3 (3 rotations)	Untethered (hard)	Surface functionalization with human immunoglobulin (HlgG) and biocompatible/Drug delivery	[178] Figure 5C
NIPAm + Bis + Irgacure 819 (photoinitiator) + Au NRs	3D (bilayer helix)	20 × 8 μm	Light/Plasmonic heating	3 (3 rotations)	Untethered (soft)	Rapid shape morphing via plasmonic heating (light)/Drug delivery	[177]
Gelatin + methacryloyl + multiferroic NPs	3D (helical)	30 μm in diameter and 100 μm in length	Rotating magnetic field	3 (3 rotations)	Untethered (soft)	Drug delivery via enzymatic biodegradability/Cell stimulation via magnetic fields	[205]

To summarize, in these past few years, most promising 4D printed microrobots have used hydrogels, LCEs, and composite materials. This section divided the smart materials into two categories: single-phase materials, which include LCEs and single-phase hydrogels, and multiphase materials containing composite materials and multiphase hydrogels produced through gray tone lithography. It is worth noting that the LCEs^[170,171] can operate in an open (air) and aqueous environment under light stimulation (fast response time). In comparison, the hydrogels require an aqueous environment and a significant change in the pH or temperature, therefore the slower response time. In addition, Jin et al.^[31] have reported that the maximal responsiveness differentiation of their hydrogels reached ≈105%, which is, according to them, larger than that reported in previous studies. Lastly, even though homogeneous materials have better printing

processability, they lack in versatility. By contrast, composite materials provide better structural integrity, magnetic abilities, and conductivity, among other features. Such features and more combined with sophisticated designs are required to reach the next generation of microrobots. Some of the first examples of this kind of microrobots are given in the following section.

5. Current State of 4D Printed Microrobotics

As described in previous sections, the TPP process provides great versatility for the design and optimization of smart microrobotics due to its inherent capability of fabricating complex 3D structures and the large number of materials that can be used. The large range of printing materials and the high degree of customization

Table 5. Summary of 4D printed structures (building blocks) using TPP fabrication. The applications and functionality can be leveraged to design and fabricate the next generation of multi-DoF microrobots.

Material composition	Geometry	Size	Stimulus	Number of DoF	Robotic system/ active continuous deformation	Stimulus response/task	Ref.
PNIPAM	2D (cantilever)	≈40 × 6 μm	Light	1	Tethered (soft)/ Yes	Swelling and shrinking (shape-changing)/ Manipulation	[169] Figure 4A
IP-DIP + LCE	2D (four orthogonal fingers)	200 × 200 × 20 μm	Light	1	Tethered (soft)/ Yes	Swelling and shrinking (shape-changing)/ Grasping	[170]
IP-DIP + LCE	3D (four-legged walker)	100 × 50 × 10 μm	Light	2 (1 translation + 1 rotation)	Untethered (soft)/ Yes	Swelling and shrinking (stick-slip)/Manipulation	[171]
EMK + Aac + NIPAAm + DPEPA	3D (hollow sphere)	60 μm diameter	Environment pH	1	Untethered (soft)/ Yes	Swelling and shrinking (shape-changing)/ Grasping, drug intake (biomedical)	[31]
–	3D (hollow cylinder)	50 μm in diameter and 200 μm in length	–	–	–	–	–
–	3D (umbrella)	≈60 μm	–	–	–	–	–
EMK + Aac + NIPAAm + DPEPA	3D (humanoid robot, race car)	≈300 × 400 × 400 μm	Environment pH	1	Untethered (soft)/ Yes	Swelling and shrinking (shape-changing)/Shape- shifting	[32] Figure 6E
pH-responsive (poly(AAc- co-AAm))/temperature- responsive (PNIPAAm)	2D (circles, squares, arrows)	≈25 × 20 × 10 μm	Environment pH/Heat	1	Untethered (soft)/ Yes	Swelling and shrinking (shape-changing)/ Manipulation	[206]
Poly(AAm-AMPS)	2D (two-armed hydrogel microcantilever manipulator)	≈30 × 17 × 1 μm	Environment pH	1	Tethered (soft)/ Yes	Swelling and shrinking (shape-changing)/ Grasping	[194] Figure 6C
PEGDA + Glycerol + CEA + photoinitiator	3D (pyramid/dome)	30 × 15 μm	Environment pH	1	Untethered (soft)/ Yes	Swelling and shrinking (shape-changing)/ Biodegradability and biosensing	[150] Figure 6B
AAc + NIPAM + PVP + TEA + DMF + C21H28N2O + C28H34O13	3D (botanical-inspired leaf and circular cage)	≈60 μm footprint	Environment pH	1	Untethered (soft)/ Yes	Swelling and shrinking (shape-changing)/selective caging of micro-objects	[148] Figure 6D

in the printing process itself allow for the fabrication of multi-DoF microrobots. Therefore, the design of 4D printed microrobots using TPP has gained large attention lately, especially in the biomedical field, due to the availability of an array printable biocompatible materials. In this section, different microrobot designs will be discussed as well as basic motion primitives designs, and promising techniques for the future of 4D printed microrobots.

In general, 4D printed microrobots consist of a 3D structure (spatially) which is able to change its properties over time (fourth dimension), such as mechanical properties and shape, which may or may not be triggered by an external stimulus. In addition, it is important that these microrobots have a tool capable of interacting with its surrounding environment, other than simple locomotion.

Sun et al. developed a hydrogel-based microrobot consisting of rigid cylinders attached by compliant springs, which is magnetically actuated using an oscillating magnetic field (Figure 5A).^[172] This microrobot is composed of a combination of PEGDA,

pentaerythritol triacrylate (PETA), and Fe₃O₄ magnetic NPs, which makes it biocompatible, biodegradable, and provides magnetic actuation. The PETA was added to enhance the structural integrity of the overall structure. As the microrobot is biodegradable within 24 h (water cleaved), one of its main applications includes targeted drug delivery. Ceylan et al. have demonstrated a hydrogel-based microswimmer using iron oxide magnetic particles that is able to undergo magnetic manipulation and is enzymatically degradable, using matrix metalloproteinase-2 (MMP-2) as a biomarker to cause microrobot swelling releasing the drug payload.^[173] Tottori et al. used a combination of clever design and magnetic actuation provided by metal coating methods to manipulate microobjects using a helical microrobot with a modified head structure,^[157] as shown in Figure 5B.

Bozuyuk et al. developed a magnetic propelled microswimmer that is made out of chitosan, a natural polymer derivative, for biocompatibility and biodegradability, superparamagnetic iron oxide NPs (SPIONs) for locomotion, and doxorubicin, a

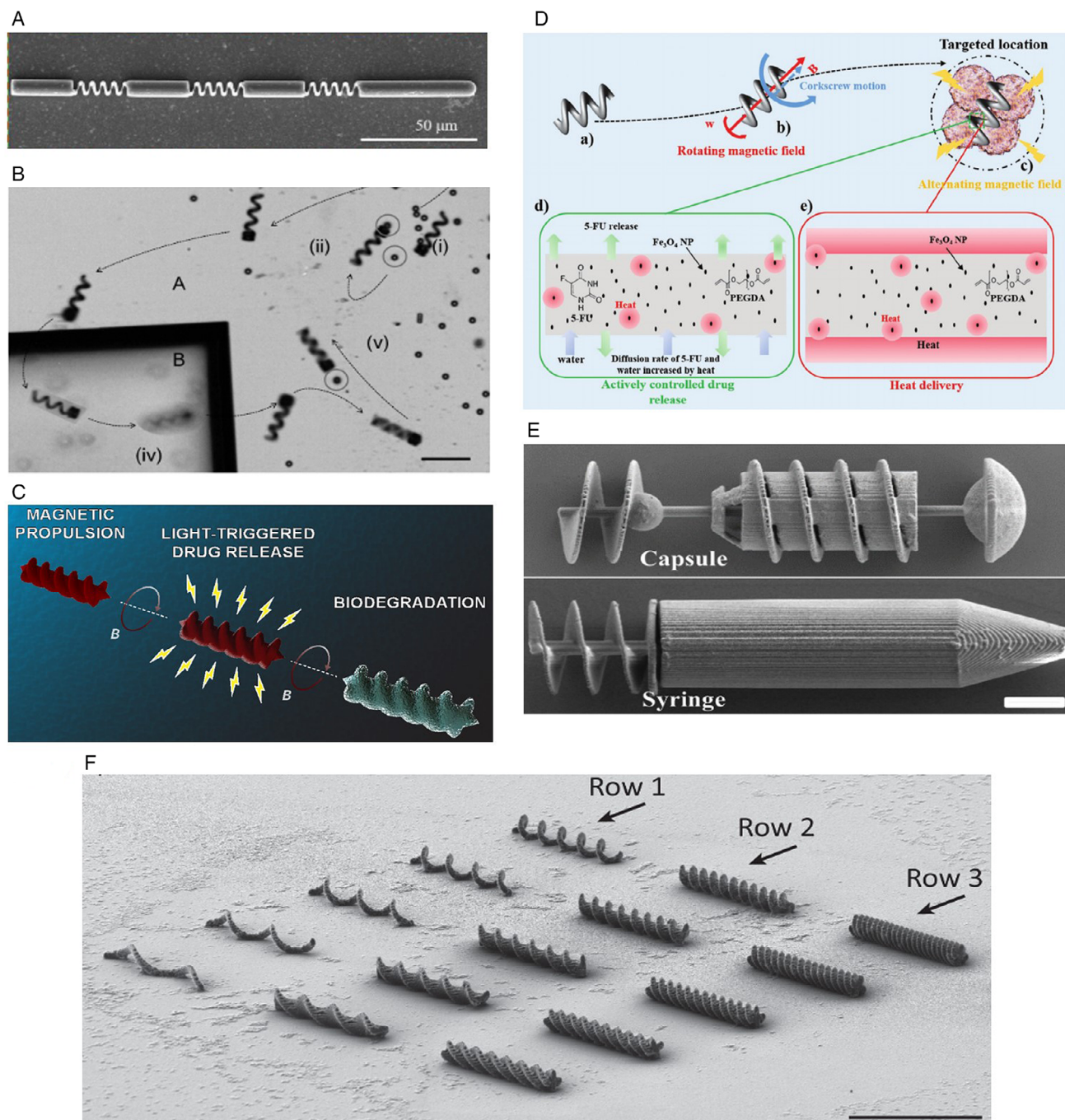


Figure 5. A few examples of 4D printed microrobots with interesting properties, responses, and applications. A) Uses undulatory motion and rigid/compliant structures to move. Reproduced with permission.^[172] Copyright 2020, MDPI. B) Microrobot with head capable of manipulating microbeads and it is fabricated with commercially available photoresists. Reproduced with permission.^[157] Copyright 2012, Wiley. C) Magnetic propulsion and light-based drug release and biodegradation. Reproduced with permission.^[174] Copyright 2018, American Chemical Society. D) Uses a rotating magnetic field for locomotion and an alternating magnetic field to trigger drug release. Reproduced with permission.^[175] Copyright 2019, Wiley. E) Creates a microvortex to absorb particles, move to a different location, and release. Reproduced with permission.^[176] Copyright 2015, Wiley. F) Comparison between helical, single, and double-twist design on magnetic microrobot with surface functionalized with human immunoglobulin (HIgG) and biocompatible. Reproduced with permission.^[178] Copyright 2014, Wiley.

chemotherapeutic drug, for drug delivery (Figure 5C).^[174] This architecture presents light-triggered drug delivery, which can be implemented in the future on a multi-DoF system in which

there are multiple different triggers for different tasks, resulting in a high precision, efficient, and versatile 4D printed microrobot.

As shown in Table 3 and Figure 5, most 4D printed structures use magnetic actuation because it is a wireless method that can provide high degree of control along with the possibility to be used in biomedical applications, especially for in vivo studies. Furthermore, magnetic fields can be used as an actuation method and/or as a programmed stimulus which causes a desired response in the TPP printed material. It should also be mentioned that despite the fact that some of these structures were printed using soft materials, they do not exhibit any active continuous deformation abilities. Park et al. demonstrated a biodegradable and biocompatible helical microrobot (Figure 5D) that presents corkscrew-like motion in low-Reynolds number fluid when exposed to a rotating magnetic field.^[175] When an alternating magnetic field is applied, however, the microrobot undergoes plasmonic heating, resulting in degradation and subsequent drug release. This microrobot can also be used for hyperthermia treatment, being able to raise the temperature locally and on-demand. Huang et al. have developed a TPP-printed micromachine consisting of a syringe inside a capsule which uses a magnetic field to rotate a shaft that creates a microvortex at the rear part of the device absorbing particles (Figure 5E).^[176] In addition, when the direction of the rotating magnetic field is reversed, the device's cap is opened, slowly releasing the particles in the desired location. Such a design can be used for targeted drug delivery and biopsy applications, among others.

With the high versatility of materials used for TPP fabrication, other actuation methods have also been explored for microrobotic applications. Nishiguchi et al. have developed a light-actuated microrobot made out of mainly PNIPAM and gold nanorods (AuNRs).^[177] This method takes advantage of different cross-linking densities during the fabrication process to create a helical bilayer microrobot. It undergoes plasmonic heating from the light source, causing controllable shape change in the microrobot itself, actuating it through low-Reynolds number environments.

Most 4D printed microrobot works present a helical-type shape because it has great mobility capabilities in low-Reynolds number environments, simulating in vivo applications. Helical-shaped microrobots also provide a high surface area, which is beneficial for surface functionalization and other applications that involve chemical reactions with the microrobot's surface. Peters et al. have compared the surface area of helical, single-twist, and double-twist designs for surface functionalization applications,^[178] as shown in Figure 5F. It has been shown that the double-twist design provides the higher surface area, proving itself more efficient for applications that require surface contact and chemical reactions.

Table 4 and Figure 6 show several examples of 4D printed structures that were made possible by the use of TPP, providing a wide range of applications, actuation methods, and stimuli responses. Although possessing just a single DoF, structures such as these serve as promising building blocks for the design and fabrication of the next generation of 4D printed microrobots. They offer great actuation and possibly sensing solutions, providing a basis for multi-DoF microrobots. Their novel stimulus response mechanisms can be combined with the aforementioned microrobotic systems to develop the next generation of 4D printed, multi-DoF microrobots. For instance, the bilayer cantilever developed by Jin et al.^[31] can serve as a basic unit along with other building blocks for the development of novel

microstructures. Furthermore, an extensive analysis of the printing parameters and their influence on the responsiveness of the hydrogel was performed, which is of paramount importance for further optimization and the ability to precisely and predictably tailor the printed structure to the desired application and functionality. For instance, several works use different hydrogel formulations to create complex bio-inspired 2D/3D shapes that undergo shape changing by the swelling and shrinking of specific parts of the structure. Xiong et al. developed a hydrogel-based microcantilever manipulator using swelling and shrinking properties of the material based on the environment's pH (Figure 4A). Hippler et al.^[169] developed a light-based microcantilever (Figure 4B) by using a bilayer structure and combining smart materials. Jin et al. have shown numerous 3D structures that can perform particle trapping and release based on a pH-responsive shape changing method (Figure 4C).^[31] Similarly, Hu et al. have developed a botanical-inspired leaf-like structure and circular cage that swells and shrinks based on the environment's pH, trapping and releasing particles inside its structure (Figure 4D).^[148]

Another example is Zeng et al.'s work on LCEs,^[171] in which a light-stimulated system was developed. They presented a light-powered box-shaped ($60 \times 30 \times 10 \mu\text{m}^3$) microscopic walkers. The walker's body is made of a homogeneously aligned LCE, while its four legs are 3D printed from a commercially available photoresist material, known as IP-DIP (Nanoscribe GmbH). When exposed to greenlight the walker's body contracts (by 20% in length), which makes the legs to come closer together. Then, once the light is removed, the walker's body relaxes again, inducing a step forward in a stick-slip fashion. The tilted legs of the walker ensure this stepping process, as they allow motion in a single direction, forward. The walker is able to achieve a planar locomotion behavior on a polyimide-coated glass surface with a velocity reaching 4.7 m s^{-1} , and under a chopped laser excitation of 532 nm, 50 Hz, and 10 W mm^{-2} . Martella et al.^[170] also used a combination of LCEs and commercial photoresists (IP-DIP) to fabricate a light-actuated microhand with four fingers, as shown in Figure 4E. The fingers are made of an LCE, which allows for a bending motion similar to that of a bilayer cantilever, thus ensuring gripping action. The four fingers are first fabricated separately and then assembled together using 3D printed rigid elements made of IP-DIP (pathway "A"), which can be somewhat challenging, especially with regard to the alignment of the micro-fingers. Thus, the need for a second strategy was created (pathway "B") where the microhand is fabricated in one single block. In both cases, terminal rigid elements (nails), made of IP-DIP, are printed to limit adhesion during contact of the fingers, either with the manipulated objects or between them, therefore ensuring a proper reopening of the microhand.

The main difference between the works shown in Figure 5 and 6 lies in their continuous deformation capabilities. While the first group appears to have static shapes and a lack of such capability, Figure 4 has soft bodies that can display large continuous deformations. Moving from one group to another can be seen as a leap from one generation of traditional microrobotic systems with mostly rigid bodies and 3D static shapes to another generation of microrobotic systems with soft bodies and dynamic shapes. Currently, compared with the former, the latter generation cannot be seen as genuine microrobots but rather as

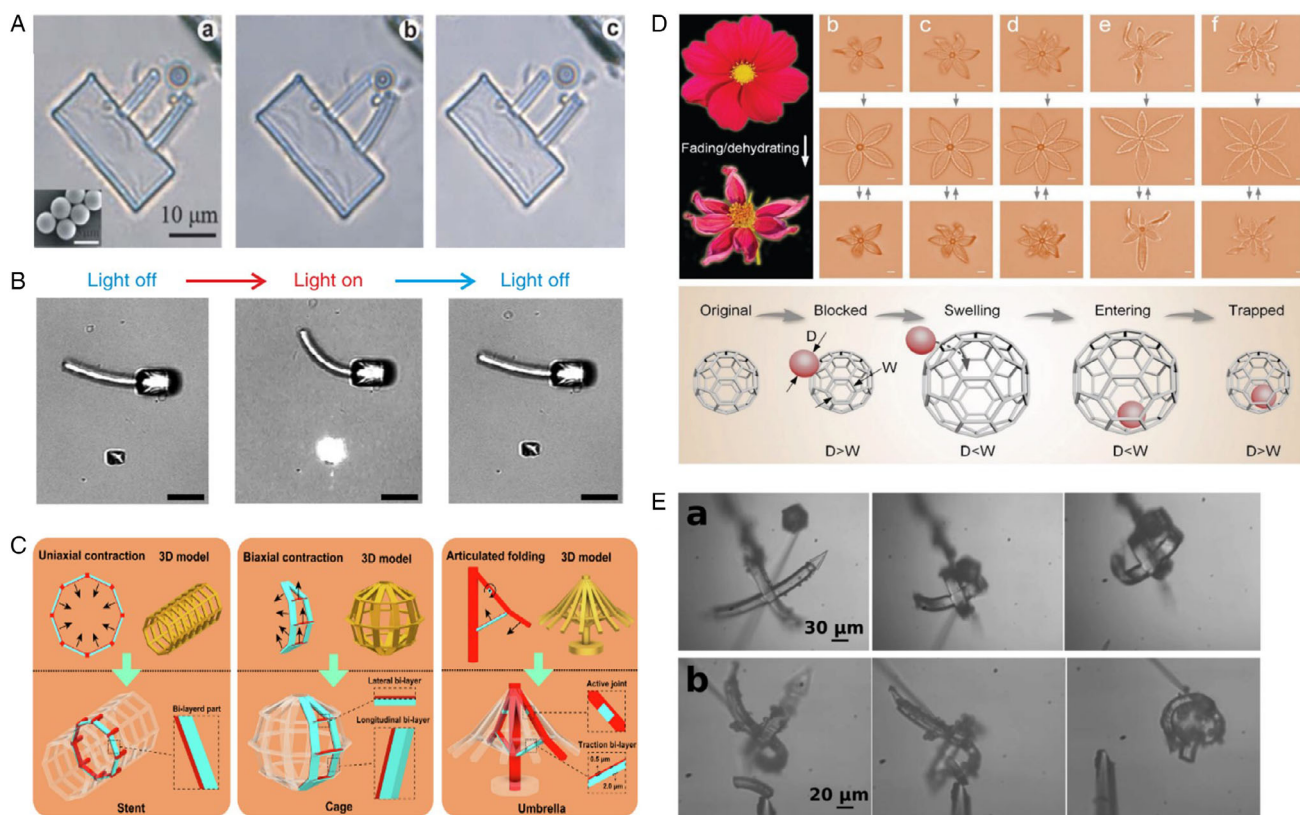


Figure 6. Examples of a few works that showcase different stimulus responses and serve as building blocks for the development of 4D printed microrobots. A) Simple grasping using a hydrogel-based gripper. Reproduced with permission.^[194] Copyright 2011, Royal Society of Chemistry. B) Light-triggered cantilever actuation. Reproduced with permission.^[169] Copyright 2019, Nature Publishing Group. C) Shape changing microstructures that optimize swelling/shrinking using bilayer cantilevers created by different printing density. Reproduced with permission.^[31] Copyright 2020, Elsevier B.V. D) Bioinspired structures capable of shape changing (pH-based) and particle trapping. Reproduced with permission.^[148] Copyright 2020, Wiley. E) Four-finger microhand. Reproduced with permission.^[170] Copyright 2017, Wiley.

building blocks, as they only have a single DoF. Nevertheless, they show great promise due to their flexibility, which allows a safer interaction with their environment and a more secure manipulation of dialect objects. In addition, their dynamic reconfigurability allows for higher dexterity and versatility.

As presented, TPP is a highly versatile method both in the fabrication capabilities and in the materials that can be used. Multiphoton absorption itself is able to create complex 3D structures with sub-100 nm resolution, and these systems allow for even more customization by the modulation of the laser power and exposure time, creating regions with different cross-linking densities. All of these fabrication properties have been explored to fabricate 4D printed microrobots with novel capabilities and multi-DoF. Furthermore, there is a wide range of possible materials for TPP, including custom-made hydrogels and commercially available photoresists. Therefore, the material selection increases even more the capabilities of the fabricated microrobots. As the physical phenomenon of two-photon absorption is well understood, numerous different material formulations for TPP exist and will be developed in the future. The combination of materials with novel properties, along with mechanical design with high control of its properties by the fabrication procedure itself, will create the next generation of 4D printed

microrobots, capable of multi-DoF actuation and sensing. Many of the works presented showcase stimulus responses that can also be used as a sensing mechanism, such as environmental pH or temperature. These sensing and actuation modalities can be combined in the future, creating a new generation of multi-DoF microrobots, especially for the biomedical field, which greatly benefits from the inherit biocompatibility of many fabrication materials. 4D printed hydrogel microstructures have demonstrated interesting active continuous deformations and shape-changing abilities. Notwithstanding the slow response time (significant change in pH or temperature is required) and the restrictions on their work environment (aqueous environment only), they represent a prime candidate for microbotic applications in the biomedical field, due in a way to their biocompatibility and soft bodies. LECs driven by light have shown great promise for microbotic applications in aqueous as well as in an open environment (air), as they have a fast response time and display high active continuous deformations. Lastly, microswimmers made from composites materials, driven by a magnetic field, which also require an aqueous (viscous) environment, were able to demonstrate high dexterity and mobility during the execution of biomedical tasks, such as cells and drug delivery. In addition, the TPP printing method is highly scalable, allowing

for high production rates of microrobots. This can be the difference that can make microrobots market-viable and result in a real impact in the biomedical fields, with applications such as microsurgery, biopsy, targeted drug delivery, and theranostics, among others.

6. Future Outlook

For the past few decades, the field of microrobotics has been developing at a fast pace and used in a wide variety of applications. With the development of novel microfabrication techniques, microrobots have moved from tethered to untethered systems with added versatility and reduced footprints. Initial microrobotic works have focused on simple solutions for actuation or sensing, which serve a purpose for narrower range of applications. Most microrobots are fabricated using planar/cleanroom techniques, which is a key design limitation because it inhibits the exploration of the third dimension and the added design complexity that comes with it. Recently, there has been a larger research focus on multi-DoF microrobotic systems, be it a combination of actuation and sensing techniques, or multiple actuation modalities on the same system, among other combinations. Following this trend, the development of more versatile, highly capable, multi-DoF microrobots is likely to happen in the near future. These microrobots will not be restricted to only a few applications but will serve more general purpose applications due to their increased number of degrees of freedom and versatility. Thus, these new mobile untethered microrobots are likely to have similar capabilities of their untethered predecessors.

As mentioned before, TPP provides a very promising solution to break the current barriers on the development of the field and will enable the fabrication of a new generation of microrobots. From a purely structural perspective, TPP allows the fabrication of complex 3D shapes and the modulation of the cross-linking density within the same structure, resulting in a fine control of how much each part of the structure can be actuated and how it responds to stimuli. Furthermore, the fabrication method can be performed with a wide variety of sensitive materials, which, in turn, can be optimized for different stimulus responses. 4D printing at its core is based on the 3D printing of stimulus responsive materials, resulting in structural changes (motion, properties, size, etc.) when triggered, giving rise to the fourth dimension, time.

Currently, the most widely used microfabrication methods, such as photolithography, are 2D based. In other words, a micro-robot or microstructure is created based on the combination of one or multiple layers with a fixed thickness. However, 4D printing techniques break this paradigm and allow the fabrication of almost arbitrary, complex 3D structures with many modes of actuation. Therefore, it provides a great opportunity for novel microrobotic designs and capabilities, but it also poses a challenge: there is a need to change the mindset when designing the next generation of microrobots to take most advantage of the 3D/4D fabrication method. As an example, 4D printing allows the fabrication of innovative mechanism-based microrobots, such as origami-based, lamina emerging mechanisms (LEMs) also referred to as “pop-up mechanisms,” and structures

that include tensional integrity (tensegrity) principles. These innovative microrobotic systems will open new challenges in modeling, parameter identification, calibration, and control.

The inherent biocompatibility of many of the materials used for TPP is a powerful tool which makes these microrobots highly suitable for biomedical applications. Some of the novel applications include targeted drug delivery, sensing and diagnosis, micro biopsy, and even minimally invasive surgery. Due to the high degree of versatility of the TPP method, there are many possible combinations of stimulus response mechanisms, actuation, and geometry, making possible the development of a wide variety of highly robust, multi-DoF microrobots for many different applications. Current actuation and responsive methods can be improved to create a robust base in which the new generation of microrobots can be built upon with the combination of novel stimulus responses, actuation methods, and structural focused design. This will result in microrobots that are extremely robust and can be used in general cases, but can be further tailored to meet a specific application requirement. This involves changing the microrobot's stimulus response based on the targeted environment, use of different drug payloads, among other small changes. In general, the future of microrobotics field relies on the development of robust and versatile multi-DoF agents, and TPP fabrication is one of the most promising fabrication methods to achieve this goal. One can also imagine the hybridation of TPP and bioprinting techniques to open the possibility of 4D printing multimaterial with various mechanical/electrical properties that can benefit microrobotics. While TPP provides a very promising method for the fabrication of complex, multi-DoF microrobots, it will also stimulate several key challenges of major interest to develop the next generation of microrobots. First, many of these materials are very soft, which makes it hard for the microrobot to apply a large range of forces without causing deformation in its structure. The inclusion of additives, such as PVP, to the fabrication materials has been shown to increase the Young's modulus of the overall material. Second, the materials used must display reversible and repeatable behavior. A purely elastic material behavior during its operation would be in contrast with today's 4D microrobots which generally present soft elasto-plastic behaviors. Purely elastic behavior will allow the implementation of more reliable control schemes making the actuation and control of the multi-DoF microrobot more robust and repeatable. To overcome this limit, the elastic behavior of the structure can result from a combination of material properties and a smart mechanism design.

Despite the many exciting opportunities and prospects for 4D printed microrobots, many challenges remain to be met. For instance, the healthcare field is a significant area of application for microrobotics; developing better and more adequate biocompatible and biodegradable 4D material is essential. Although many 4D printed polymers are generally nontoxic, the same cannot be said about monomers and photoinitiators used for the fabrication. The effect of these residual materials on living systems and their impact, in general, needs to be further investigated. Furthermore, some of the utilized materials, such as hydrogels, rely on an aqueous environment, which might limit their use and application possibilities; however, it also makes them better suited for certain applications, such as the biomedical field. In addition, despite the wide variety of 4D printed microrobots

reported, less effort has been made to explore the concept in real-world applications. Therefore, future work on the efficiency of the printing process and the performances and adaptability of the printed microrobots' response is crucial. For example, the development of advanced materials with an independent multi-response ability or genuine multimaterial 4D printed microrobots will allow for a truly spatially controlled response, thus achieving more versatility and DoFs in terms of design and actuation. Moreover, additional efforts in the study of robotic performances (positioning accuracy, repeatability, useful life, generated force, etc.) to meet key microrobotic requirements (Table 5) are needed. 4D printed microrobotics as a research field can help bring chemistry and polymer synthesis to microrobotics community through multidisciplinary projects from funding agencies worldwide, therefore contributing to the development and advancement of future micromachines (bioinspired such as Ant-Bot, Bee-Bot) and the next generation of microfactory.

There exists a gap between the potential and current state of 4D printed microrobots. Up to this point, most works in this field focus on sophisticated demonstrations of different capabilities, but real-world applications are still to be addressed. To bridge this gap, self-contained, production-ready, highly dexterous, multi-DoF microrobots which are able to sense their environment, communicate, collaborate, and even auto-degrade (when necessary) are needed. As discussed, the development of novel stimuli-responsive (smart) materials coupled with innovative designs provided by TPP fabrication techniques is of paramount importance because it is one of the most promising roads to the next generation of 4D printed microrobots. The continued development of 4D printing technologies and materials will enable the development of a new generation of smart microrobotic systems with embedded sensors and actuators, and with high adaptability for very small structures.

Acknowledgements

This work was supported by NSF NRI Award#: 1637961, NSF IIS Award#: 1763689, FACE Foundation, Thomas Jefferson Fund, EIPHI Graduate School (ANR17-EURE-0002), and Bourgogne Franche-Comté.

Conflict of Interest

The authors declare no conflict of interest.

Keywords

4D printing, additive manufacturing, microrobotics, smart materials, two-photon polymerization

Received: September 30, 2020

Revised: October 26, 2020

Published online:

- [1] I. Gibson, D. W. Rosen, B. Stucker, *Additive Manufacturing Technologies*, Vol. 17, Springer, Berlin/New York **2014**.
[2] A. Bandyopadhyay, S. Bose, *Additive Manufacturing*, CRC Press, Boca Raton, FL **2019**.

- [3] T. D. Ngo, A. Kashani, G. Imbalzano, K. T. Nguyen, D. Hui, *Composites B* **2018**, *143*, 172.
[4] W. E. Frazier, *J. Mater. Eng. Perform.* **2014**, *23*, 1917.
[5] D. Herzog, V. Seyda, E. Wycisk, C. Emmelmann, *Acta Mater.* **2016**, *117*, 371.
[6] J. Deckers, J. Vleugels, J. P. Kruth, *J. Ceram. Sci. Technol.* **2014**, *5*, 245.
[7] P. Parandoush, D. Lin, *Composite Struct.* **2017**, *182*, 36.
[8] B. Lyons, Additive Manufacturing in Aerospace; Examples and Research Outlook Introduction and Content, Technical Report, National Academy of Engineering, <http://www.ae.com/i18n/amrcorp/newsroom/fuel-smart.jsp> (accessed: June 2020).
[9] V. Juechter, M. M. Franke, T. Merenda, A. Stich, C. Körner, R. F. Singer, *Addit. Manuf.* **2018**, *22*, 118.
[10] E. Uhlmann, R. Kersting, T. B. Klein, M. F. Cruz, A. V. Borille, *Procedia CIRP* **2015**, *35*, 55.
[11] S. M. Wagner, R. O. Walton, *Prod. Plann. Control* **2016**, *27*, 1124.
[12] B. Z. Wang, Y. Chen, *Appl. Mech. Mater.* **2014**, *496–500*, 2687.
[13] H. Dodziuk, *Pol. J. Cardio Thorac. Surg.* **2016**, *3*, 283.
[14] G. M. Paul, A. Rezaenia, P. Wen, S. Condoor, N. Parkar, W. King, T. Korakianitis, Medical Applications for 3D Printing: Recent Developments, Technical Report, Saint Louis University, **2018**.
[15] W. Xu, X. Wang, N. Sandler, S. Willför, C. Xu, *ACS Sustainable Chem. Eng.* **2018**, *6*, 5663.
[16] D. Delgado Camacho, P. Clayton, W. J. O'Brien, C. Seepersad, M. Juenger, R. Ferron, S. Salamone, *Autom. Constr.* **2018**, *89*, 110.
[17] J. I. Lipton, M. Cutler, F. Nigl, D. Cohen, H. Lipson, *Trends Food Sci. Technol.* **2015**, *43*, 114.
[18] F. C. Godoi, S. Prakash, B. R. Bhandari, *J. Food Eng.* **2016**, *179*, 44.
[19] C. Schelly, G. Anzalone, B. Wijnen, J. M. Pearce, *J. Visual Lang. Comput.* **2015**, *28*, 226.
[20] H. Exner, M. Horn, A. Streek, F. Ullmann, L. Hartwig, P. Regenfuß, R. Ebert, *Virtual Phys. Prototyping* **2008**, *3*, 3.
[21] *Laser 3D Manufacturing II* (Eds: H. Exner, A. Streek, In H. Helvajian, A. Piqué, M. Wegener, B. Gu), Vol. 9353, SPIE, Bellingham, WA **2015**, p. 93530P.
[22] K. V. Wong, A. Hernandez, *ISRN Mech. Eng.* **2012**, *2012*, 1.
[23] N. Guo, M. C. Leu, *Front. Mech. Eng.* **2013**, *8*, 215.
[24] K. S. Teh, Additive Direct-Write Microfabrication for MEMS: A Review, <https://link-springer-com.ezproxy.lib.purdue.edu/article/10.1007/s11465-017-0484-4> (accessed: October 2020).
[25] F. Momeni, X. Liu, J. Ni, *Mater. Des.* **2017**, *122*, 42.
[26] A. Y. Lee, J. An, C. K. Chua, *Engineering* **2017**, *3*, 663.
[27] C. M. González-Henríquez, M. A. Sarabia-Vallejos, J. R. Hernandez, *Int. J. Mole. Sci.* **2019**, *20*, 5.
[28] Z. X. Khoo, J. E. M. Teoh, Y. Liu, C. K. Chua, S. Yang, J. An, K. F. Leong, W. Y. Yeong, *Virtual Phys. Prototyping* **2015**, *10*, 103.
[29] Y. Xia, Y. He, F. Zhang, Y. Liu, J. Leng, *Adv. Mater.* **2020**, 2000713.
[30] J. del Barrio, C. Sánchez-Somolinos, *Adv. Opt. Mater.* **2019**, *7*, 16.
[31] D. Jin, Q. Chen, T. Y. Huang, J. Huang, L. Zhang, H. Duan, *Mater. Today* **2020**, *32*, 19.
[32] T.-Y. Huang, H.-W. Huang, D. D. Jin, Q. Y. Chen, J. Y. Huang, L. Zhang, H. L. Duan, *Sci. Adv.* **2020**, *6*, 3.
[33] J.-H. Youn, S. M. Jeong, G. Hwang, H. Kim, K. Hyeon, J. Park, K.-U. Kyung, *Appl. Sci.* **2020**, *10*, 610.
[34] M. Attaran, *Bus. Horizons* **2017**, *60*, 677.
[35] S. Lim, R. A. Buswell, T. T. Le, S. A. Austin, A. G. Gibb, T. Thorpe, *Autom. Constr.* **2012**, *21*, 262.
[36] M. Vaezi, H. Seitz, S. Yang, *Int. J. Adv. Manuf. Technol.* **2013**, *67*, 1721.
[37] C. A. Spiegel, M. Hippler, A. Münchinger, M. Bastmeyer, C. Barner Kowollik, M. Wegener, E. Blasco, *Adv. Funct. Mater.* **2020**, *30*, 1907615.
[38] C. de Marco, C. C. J. Alcântara, S. Kim, F. Briatico, A. Kadioglu, G. de Bernardis, X. Chen, C. Marano, B. J. Nelson, S. Pané, *Adv. Mater. Technol.* **2019**, *4*, 1900332.

- [39] B. J. Nelson, L. Dong, F. Arai, *Springer Handbook of Robotics*, Springer, Berlin Heidelberg **2008**, pp. 411–450.
- [40] E. Diller, M. Sitti, *Micro-Scale Mobile Robotics*, Now Publishers, Delft **2013**.
- [41] D. L. Hu, B. Chan, J. W. Bush, *Nature* **2003**, 424, 663.
- [42] G. P. Sutton, M. Burrows, *J. Exp. Biol.* **2011**, 214, 836.
- [43] M. Wautelet, *Euro. J. Phys.* **2001**, 22, 601.
- [44] B. J. Nelson, I. K. Kaliakatsos, J. J. Abbott, *Annu. Rev. Biomed. Eng.* **2010**, 12, 55.
- [45] J. Li, B. Esteban-Fernández de Ávila, W. Gao, L. Zhang, J. Wang, *Sci. Robot.* **2017**, 2, 4.
- [46] Y. Kim, G. A. Parada, S. Liu, X. Zhao, *Sci. Robot.* **2019**, 4, 7329.
- [47] S. Jeon, A. K. Hoshiar, K. Kim, S. Lee, E. Kim, S. Lee, J. Y. Kim, B. J. Nelson, H. J. Cha, B. J. Yi, H. Choi, *Soft Robot.* **2019**, 6, 54.
- [48] S. Martel, M. Mohammadi, O. Felfoul, Z. Lu, P. Poupponeau, *Int. J. Robot. Res.* **2009**, 28, 571.
- [49] W. Hu, G. Z. Lum, M. Mastrangeli, M. Sitti, *Nature* **2018**, 554, 81.
- [50] X. Wu, J. Liu, C. Huang, M. Su, T. Xu, *IEEE Trans. Autom. Sci. Eng.* **2020**, 17, 823.
- [51] J. Leclerc, H. Zhao, D. Z. Bao, A. T. Becker, M. Ghosn, D. J. Shah, Agile 3D-Navigation of a Helical Magnetic Swimmer, Technical Report.
- [52] W. Jing, N. Pagano, D. J. Cappelleri, *J. Micro-Bio Robot.* **2013**, 8, 1.
- [53] F. Ullrich, C. Bergeles, J. Pokki, O. Ergeneman, S. Erni, G. Chatzipiripiridis, S. Pané, C. Framme, B. J. Nelson, *Invest. Ophthalmol. Visual Sci.* **2013**, 54, 2853.
- [54] X. Liu, J. Shi, Z. Zong, K. T. Wan, Y. Sun, *Ann. Biomed. Eng.* **2012**, 40, 2122.
- [55] M. Medina-Sánchez, L. Schwarz, A. K. Meyer, F. Hebenstreit, O. G. Schmidt, *Nano Lett.* **2016**, 16, 555.
- [56] P. Sakti, A. Treimanis, P. Fardim, P. Ronkanen, P. Kallio, in *IEEE/RSJ Int. Conf. on Intelligent Robots and Systems (IROS)*, IEEE, Taipei **2010**, pp. 5762–5767.
- [57] J. Liu, J. Wen, Z. Zhang, H. Liu, Y. Sun, *Microsyst. Nanoeng.* **2015**, 1, 1.
- [58] T. G. Leong, C. L. Randall, B. R. Benson, N. Bassik, G. M. Stern, D. H. Gracias, *Proc. Natl. Acad. Sci.* **2009**, 106, 703.
- [59] T. Fischer, A. Agarwal, H. Hess, *Nat. Nanotechnol.* **2009**, 4, 162.
- [60] N. Bassik, A. Brafman, A. M. Zarafshar, M. Jamal, D. Luvsanjav, F. M. Selaru, D. H. Gracias, *J. Am. Chem. Soc.* **2010**, 132, 16314.
- [61] S. K. Verma, R. Chauhan, *Indian J. Dent.* **2014**, 5, 62.
- [62] S. Gupta, K. Ramesh, S. Ahmed, V. Kakkar, *Int. J. Bio-Sci. Bio-Technol.* **2016**, 8, 311.
- [63] A. T. Giannitsis, *Est. J. Eng.* **2011**, 17, 2.
- [64] M. A. Miled, M. Sawan, *IEEE Trans. Biomed. Circuits Syst.* **2012**, 6, 120.
- [65] M. Kharboutly, A. Melis, M. Gauthier, N. Chaillet, in *2012 IEEE Int. Conf. on Automation Science and Engineering (CASE)*, IEEE, Seoul **2012**, pp. 950–955.
- [66] T. Michálek, A. Bolopion, Z. Hurák, M. Gauthier, *Phys. Rev. E* **2019**, 99, 5.
- [67] D. Xu, K. Shou, B. J. Nelson, *Microelectron. Eng.* **2011**, 88, 2703.
- [68] A. Subramanian, B. Vikramaditya, L. Dong, D. Bell, R. J. Nelson, *Robotics: Science and Systems*, Vol. 1, Robotics: Science and Systems Foundation **2005**, pp. 327–334.
- [69] C. Iliescu, G. Tresset, L. Yu, G. Xu, 3D Dielectrophoretic Chips: Trapping and Separation of Cell Populations, Technical Report 1 **2010**.
- [70] H. K. Chu, Z. Huan, J. K. Mills, J. Yang, D. Sun, *Lab Chip* **2015**, 15, 920.
- [71] M. Fouet, S. Cargou, R. Courson, X. Bouquet, L. Salvagnac, A. Gue, in *Int. Conf. on Solid-State Sensors, Actuators and Microsystems (Transducers)*, IEEE, Anchorage, AK **2015**, pp. 529–532.
- [72] H. Chetouani, C. Jeandey, V. Haguët, H. Rostaing, C. Dieppedale, G. Reyne, in *12th Biennial IEEE Conf. on Electromagnetic Field Computation*, IEEE, Miami, FL **2006**, pp. 445–445.
- [73] W. C. Nelson, C.-J. Kim, *J. Adhes. Sci. Technol.* **2012**, 26, 1747.
- [74] S. Thalhammer, A. Wixforth, *J. Biosens. Bioelectron.* **2013**, 4, 13.
- [75] W. Duan, W. Wang, S. Das, V. Yadav, T. E. Mallouk, A. Sen, *Annu. Rev. Anal. Chem.* **2015**, 8, 311.
- [76] Y. Ghallab, W. Badawy, *IEEE Circuits Syst. Mag.* **2004**, 4, 5.
- [77] B. Brazey, J. Cottet, A. Bolopion, H. Van Lintel, P. Renaud, M. Gauthier, *Lab Chip* **2018**, 18, 818.
- [78] R. Arvidsson, S. F. Hansen, *Environ. Sci.: Nano* **2020**, 7, 2875.
- [79] E. Denkhaus, K. Salnikow, *Crit. Rev. Oncol./Hematol.* **2002**, 42, 35.
- [80] S. N. Luoma, O. Woodrow, W. Plaza, L. H. Hamilton, R. B. Cook, D. E. Garcia, B. S. Gelb, S. R. Gerber, C. L. Glazer, S. Hutchison, I. E. Sanchez, Silver Nanotechnologies and the Environment: Old Problems or New Challenges, Technical Report, www.pewtrusts.org (accessed: October 2020).
- [81] S. Surana, A. R. Shenoy, Y. Krishnan, *Nat. Nanotechnol.* **2015**, 10, 741.
- [82] V. Iacovacci, L. Ricotti, E. Sinibaldi, G. Signore, F. Vistoli, A. Menciasci, *Adv. Sci.* **2018**, 5, 9.
- [83] N. Weber, H. Zappe, A. Seifert, *J. Microelectromech. Syst.* **2012**, 21, 1357.
- [84] S. Bargiel, K. Rabenorosoa, C. Clévy, C. Gorecki, P. Lutz, *J. Micromechan. Microeng.* **2010**, 20, 4.
- [85] K. Aoki, H. T. Miyazaki, H. Hirayama, K. Inoshita, T. Baba, K. Sakoda, N. Shinya, Y. Aoyagi, *Nat. Mater.* **2003**, 2, 117.
- [86] J.-Y. Rauch, O. Lehmann, P. Rougeot, J. Abadie, J. Agnus, M. A. Suarez, *J. Vac. Sci. Technol. A* **2018**, 36, 041601.
- [87] N. N. Sharma, R. K. Mittal, *Int. J. Smart Sens. Intell. Syst.* **2008**, 1, 1.
- [88] V. Placet, M. Blot, T. Weemaes, H. Bernollin, G. Laurent, F. Amiot, C. Clévy, J. Beaugrand, *Mater. Today: Proc.* **2020**, 31, S3030.
- [89] Y. Wei, Q. Xu, *IEEE Trans. Autom. Sci. Eng.* **2019**, 16, 931.
- [90] H. Bettahar, O. Lehmann, C. Clévy, N. Courjal, P. Lutz, *IEEE/ASME Trans. Mechatronics* **2020**, 25, 616.
- [91] V. Guelpa, A. V. Kudryavtsev, N. L.-F. Piat, S. Dembele, in *2018 Int. Conf. on Manipulation, Automation and Robotics at Small Scales (MARSS)*, IEEE, Nagoya **2018**, pp. 1–6.
- [92] O. Ozguner, T. Shkurti, S. Huang, R. Hao, R. C. Jackson, W. S. Newman, M. C. Cavusoglu, *IEEE Trans. Autom. Sci. Eng.* **2020**, 30, 1.
- [93] M. Al Janaideh, M. Al Saaideh, M. Rakotondrabe, *Mech. Syst. Signal Process.* **2020**, 145, 106880.
- [94] Q. Xu, *IEEE Trans. Indus. Electron.* **2020**, 1.
- [95] C. Clévy, M. Rakotondrabe, N. Chaillet, *Signal Measurement and Estimation Techniques for Micro and Nanotechnology*, Springer, New York, NY **2011**.
- [96] H. Bettahar, C. Clévy, N. Courjal, P. Lutz, *IEEE Robot. Autom. Lett.* **2020**, 5, 6396.
- [97] M. Power, A. J. Thompson, S. Anastasova, G. Z. Yang, *Small* **2018**, 14, 16.
- [98] W. Haouas, R. Dahmouche, N. Piat, G. Laurent, N. Le Fort-Piat, G. J. Laurent, *Am. Soc. Mech. Eng.* **2018**, 10, 1.
- [99] H. McClintock, F. Z. Temel, N. Doshi, J.-S. Koh, R. J. Wood, *Sci. Robot.* **2018**, 3, 14.
- [100] A. Homayouni-Amlashi, A. Mohand-Ousaid, M. Rakotondrabe, *J. Micro-Bio Robot.* **2020**, 16, 65.
- [101] C. Pawashe, S. Floyd, E. Diller, M. Sitti, *IEEE Trans. Robot.* **2012**, 28, 467.
- [102] W. Jing, D. Cappelleri, *Robotics* **2014**, 3, 106.
- [103] A. Barbot, D. Decanin, G. Hwang, in *IEEE/RSJ Int. Conf. on Intelligent Robots and Systems*, IEEE, Chicago, IL **2014**, pp. 4662–4667.

- [104] M. Dkhil, M. Kharboutly, A. Bolopion, S. Regnier, M. Gauthier, *IEEE Trans. Autom. Sci. Eng.* **2017**, *14*, 1387.
- [105] H. Jia, E. Mailand, J. Zhou, Z. Huang, G. Dietler, J. M. Kolinski, X. Wang, M. S. Sakar, *Small* **2019**, *15*, 4.
- [106] S. Palagi, A. G. Mark, S. Y. Reigh, K. Melde, T. Qiu, H. Zeng, C. Parmeggiani, D. Martella, A. Sanchez-Castillo, N. Kapernaum, F. Giesselmann, D. S. Wiersma, E. Lauga, P. Fischer, *Nat. Mater.* **2016**, *15*, 647.
- [107] T. Qiu, S. Palagi, A. G. Mark, K. Melde, F. Adams, P. Fischer, *Appl. Phys. Lett.* **2016**, *109*, 19.
- [108] J. Matouš, A. Kollarčík, M. Gurtner, T. Michálek, Z. Hurák, *IFAC-PapersOnLine* **2019**, *52*, 483.
- [109] F. Guo, Z. Mao, Y. Chen, Z. Xie, J. P. Lata, P. Li, L. Ren, J. Liu, J. Yang, M. Dao, S. Suresh, T. J. Huang, *Proc. Natl. Acad. Sci.* **2016**, *113*, 1522.
- [110] A. Ozcelik, J. Rufo, F. Guo, Y. Gu, P. Li, J. Lata, T. J. Huang, *Nat. Methods* **2018**, *15*, 1021.
- [111] X. Tao, T. D. Nguyen, H. Jin, R. Tao, J. Luo, X. Yang, H. Torun, J. Zhou, S. Huang, L. Shi, D. Gibson, M. Cooke, H. Du, S. Dong, J. Luo, Y. Q. Fu, *Sens. Actuators, B* **2019**, *299*, 126991.
- [112] L. Ren, N. Nama, J. M. McNeill, F. Soto, Z. Yan, W. Liu, W. Wang, J. Wang, T. E. Mallouk, *Sci. Adv.* **2019**, *5*, 10.
- [113] A. Barbot, D. Decanini, G. Hwang, *Sci. Rep.* **2016**, *6*, 19041.
- [114] A. Oulmas, N. Andreff, S. Régnier, *Int. J. Robot. Res.* **2018**, *37*, 1.
- [115] C. Pawashe, S. Floyd, M. Sitti, *Appl. Phys. Lett.* **2009**, *94*, 16.
- [116] M. Salehizadeh, E. Diller, *Int. J. Robot. Res.* **2020**, *39*, 1377.
- [117] E. Diller, J. Giltinan, M. Sitti, *Int. J. Robot. Res.* **2013**, *32*, 614.
- [118] S. Chowdhury, W. Jing, D. J. Cappelleri, *Micromachines* **2016**, *7*, 1.
- [119] A. W. Mahoney, N. D. Nelson, K. E. Peyer, B. J. Nelson, J. J. Abbott, *Appl. Phys. Lett.* **2014**, *104*, 14.
- [120] S. Tottori, N. Sugita, R. Kometani, S. Ishihara, M. Mitsuishi, *J. Micro-Nano Mechatronics* **2011**, *6*, 89.
- [121] A. Ashkin, J. M. Dziedzic, T. Yamane, *Nature* **1987**, *330*, 769.
- [122] M. Yin, E. Gerena, S. Regnier, C. Pacoret, in *2016 Int. Conf. on Manipulation, Automation and Robotics at Small Scales (MARSS)*, IEEE, Paris **2016**, pp. 1–7.
- [123] P. J. Rodrigo, L. Kelemen, C. A. Alonzo, I. R. Perch-Nielsen, J. S. Dam, P. Ormos, J. Glückstad, *Opt. Express* **2007**, *15*, 14.
- [124] S. Hu, H. Xie, T. Wei, S. Chen, D. Sun, *Appl. Sci.* **2019**, *9*, 2883.
- [125] E. Avci, M. Grammatikopoulou, G. Z. Yang, *Adv. Opt. Mater.* **2017**, *5*, 19.
- [126] Y. Tanaka, *Opt. Lasers Eng.* **2018**, *111*, 65.
- [127] F. Arai, K. Yoshikawa, T. Sakami, T. Fukuda, *Appl. Phys. Lett.* **2004**, *85*, 4301.
- [128] H. Chen, C. Wang, Y. Lou, *IEEE Trans. Biomed. Eng.* **2013**, *60*, 1518.
- [129] E. Gerena, S. Régnier, S. Haliyo, S. H. High, *IEEE Robot. Autom. Lett.* **2019**, *2*, 647.
- [130] R. H. Farahi, A. Passian, T. L. Ferrell, T. Thundat, *Appl. Phys. Lett.* **2004**, *85*, 4237.
- [131] J. G. Ortega-Mendoza, J. A. Sarabia-Alonso, P. Zaca-Morán, A. Padilla-Vivanco, C. Toxqui-Quitl, I. Rivas-Camero, J. Ramirez-Ramirez, S. A. Torres-Hurtado, R. Ramos-García, *Opt. Express* **2018**, *26*, 6653.
- [132] E. Vela, M. Hafez, S. Régnier, *Int. J. Optomechatronics* **2009**, *3*, 289.
- [133] R. T. Mallea, A. Bolopion, J. C. Beugnot, P. Lambert, M. Gauthier, *IEEE/ASME Trans. Mechatronics* **2018**, *23*, 1543.
- [134] R. T. Mallea, A. De Maeijer, A. Bolopion, M. Gauthier, M. Kinnaert, P. Lambert, *J. Micro-Bio Robot.* **2019**, *15*, 13.
- [135] M. Sitti, D. S. Wiersma, *Adv. Mater.* **2020**, *32*, 1906766.
- [136] J. Yang, C. Zhang, X. Wang, W. Wang, N. Xi, L. Liu, *Sci. China Technol. Sci.* **2019**, *62*, 1.
- [137] C. Pacchierotti, S. Scheggi, D. Prattichizzo, S. Misra, *Front. Robot. AI* **2016**, *3*.
- [138] M. B. Popovic, *Biomechatronics*, Academic Press, Cambridge, MA **2019**.
- [139] C. A. Mack, *Emerging Lithographic Technologies VIII (SPIE)*, Vol. 5374, International SPIE, Bellingham, WA **2004**, pp. 1–8.
- [140] V. R. Manfrinato, L. Zhang, D. Su, H. Duan, R. G. Hobbs, E. A. Stach, K. K. Berggren, *Nano Lett.* **2013**, *13*, 1555.
- [141] V. R. Manfrinato, J. Wen, L. Zhang, Y. Yang, R. G. Hobbs, B. Baker, D. Su, D. Zakharov, N. J. Zaluzec, D. J. Miller, E. A. Stach, K. K. Berggren, *Nano Lett.* **2014**, *14*, 4406.
- [142] I. Sakellari, E. Kabouraki, D. Gray, V. Purlys, C. Fotakis, A. Pikulin, N. Bituryn, M. Vamvakaki, M. Farsari, *ACS Nano* **2012**, *6*, 2302.
- [143] H. W. Huang, M. S. Sakar, A. J. Petruska, S. Pané, B. J. Nelson, *Nat. Commun.* **2016**, *7*, 1.
- [144] R. Raman, B. Bhaduri, M. Mir, A. Shkumatov, M. K. Lee, G. Popescu, H. Kong, R. Bashir, *Adv. Healthcare Mater.* **2016**, *5*, 610.
- [145] A. Ovsianikov, B. N. Chichkov, *Nanoelectronics and Photonics*, Springer, New York, NY **2008**, pp. 427–446.
- [146] Q. Geng, D. Wang, P. Chen, S. C. Chen, *Nat. Commun.* **2019**, *10*, 1.
- [147] J. Purto, A. Verch, P. Rogin, R. Hensel, *Microelectron. Eng.* **2018**, *194*, 45.
- [148] Y. Hu, Z. Wang, D. Jin, C. Zhang, R. Sun, Z. Li, K. Hu, J. Ni, Z. Cai, D. Pan, X. Wang, W. Zhu, J. Li, D. Wu, L. Zhang, J. Chu, *Adv. Funct. Mater.* **2020**, *30*, 1907377.
- [149] D. Schwärzle, X. Hou, O. Prucker, J. Rühle, *Adv. Mater.* **2017**, *29*, 1703469.
- [150] E. Scarpa, E. D. Lemma, R. Fiammengo, M. P. Cipolla, F. Pisanello, F. Riczi, M. De Vittorio, *Sens. Actuators, B* **2019**, *279*, 418.
- [151] Y. Tian, Y. L. Zhang, H. Xia, L. Guo, J. F. Ku, Y. He, R. Zhang, B. Z. Xu, Q. D. Chen, H. B. Sun, *Phys. Chem. Chem. Phys.* **2011**, *13*, 4835.
- [152] Z. Xiong, X. Z. Dong, W. Q. Chen, X. M. Duan, *Appl. Phys. A: Mater. Sci. Process.* **2008**, *93*, 447.
- [153] T. Watanabe, M. Akiyama, K. Totani, S. Kuebler, F. Stellacci, W. Wenseleers, K. Braun, S. Marder, J. Perry, *Adv. Funct. Mater.* **2002**, *12*, 611.
- [154] A. Tudor, H. Zhang, A. J. Thompson, V. F. Curto, A. Tudor, C. Delaney, H. Zhang, A. J. Thompson, V. F. Curto, G. Yang, M. J. Higgins, *Mater. Today* **2018**, *21*, 807.
- [155] H. Zeng, D. Martella, P. Wasylczyk, G. Cerretti, J. C. G. Lavocat, C. H. Ho, C. Parmeggiani, D. S. Wiersma, *Adv. Mater.* **2014**, *26*, 2319.
- [156] F. Qiu, L. Zhang, K. E. Peyer, M. Casarosa, A. Franco-Obregón, H. Choi, B. J. Nelson, *J. Mater. Chem. B* **2014**, *2*, 357.
- [157] S. Tottori, L. Zhang, F. Qiu, K. K. Krawczyk, A. Franco-Obregón, B. J. Nelson, *Adv. Mater.* **2012**, *24*, 811.
- [158] C. A. Koepele, M. Guix, C. Bi, G. Adam, D. J. Cappelleri, *Adv. Intell. Syst.* **2020**, *2*, 1900147.
- [159] C. L. Lay, Y. H. Lee, M. R. Lee, I. Y. Phang, X. Y. Ling, *ACS Appl. Mater. Interfaces* **2016**, *8*, 8145.
- [160] E. C. Spivey, E. T. Ritschdorff, J. L. Connell, C. A. McLennon, C. E. Schmidt, J. B. Shear, *Adv. Funct. Mater.* **2013**, *23*, 333.
- [161] X. Wang, Z. Wei, C. Z. Baysah, M. Zheng, J. Xing, *RSC Adv.* **2019**, *9*, 34472.
- [162] Y. Liu, W. Xiong, L. J. Jiang, Y. S. Zhou, Y. F. Lu, *Laser 3D Manufacturing III*, Vol. 9738, SPIE, Bellingham, WA **2016**.
- [163] U. Staudinger, G. Zyla, B. Krause, A. Janke, D. Fischer, C. Esen, B. Voit, A. Ostendorf, *Microelectron. Eng.* **2017**, *179*, 48.
- [164] E. Blasco, J. Müller, P. Müller, V. Trouillet, M. Schön, T. Scherer, C. Barner-Kowollik, M. Wegener, *Adv. Mater.* **2016**, *28*, 3592.
- [165] R. Nakamura, K. Kinashi, W. Sakai, N. Tsutsumi, *Phys. Chem. Chem. Phys.* **2016**, *18*, 17024.
- [166] T. Jonavicius, S. Rekstyte, M. Malinauskas, *Lith. J. Phys.* **2014**, *54*, 162.

- [167] A. Marino, J. Barsotti, G. De Vito, C. Filippeschi, B. Mazzolai, V. Piazza, M. Labardi, V. Mattoli, G. Ciofani, *ACS Appl. Mater. Interfaces* **2015**, 7, 25574.
- [168] D. Kim, Z. Hao, J. Ueda, A. Ansari, *J. Micromech. Microeng.* **2019**, 29, 105006.
- [169] M. Hippler, E. Blasco, J. Qu, M. Tanaka, C. Barner-Kowollik, M. Wegener, M. Bastmeyer, *Nat. Commun.* **2019**, 10, 1.
- [170] D. Martella, S. Nocentini, D. Nuzhdin, C. Parmeggiani, D. S. Wiersma, *Adv. Mater.* **2017**, 29, 42.
- [171] H. Zeng, P. Wasylczyk, C. Parmeggiani, D. Martella, M. Burresti, D. S. Wiersma, *Adv. Mater.* **2015**, 27, 3883.
- [172] H. C. M. Sun, P. Liao, T. Wei, L. Zhang, D. Sun, *Micromachines* **2020**, 11, 4.
- [173] H. Ceylan, I. C. Yasa, O. Yasa, A. F. Tabak, J. Giltinan, M. Sitti, *ACS Nano* **2019**, 13, 3353.
- [174] U. Bozuyuk, O. Yasa, I. C. Yasa, H. Ceylan, S. Kizilel, M. Sitti, *ACS Nano* **2018**, 12, 9617.
- [175] J. Park, C. Jin, S. Lee, J. Kim, H. Choi, *Adv. Healthcare Mater.* **2019**, 8, 1900213.
- [176] T.-Y. Huang, M. S. Sakar, A. Mao, A. J. Petruska, F. Qiu, X.-B. Chen, S. Kennedy, D. Mooney, B. J. Nelson, *Adv. Mater.* **2015**, 27, 6644.
- [177] A. Nishiguchi, H. Zhang, S. Schweizerhof, M. F. Schulte, A. Mourran, M. Möller, *ACS Appl. Mater. Interfaces* **2020**, 12, 12176.
- [178] C. Peters, O. Ergeneman, P. D. W. Garcia, M. Müller, S. Pané, B. J. Nelson, C. Hierold, *Adv. Funct. Mater.* **2014**, 24, 5269.
- [179] Z. Wang, A. A. Volinsky, N. D. Gallant, *J. Appl. Polym. Sci.* **2014**, 131, 41050.
- [180] L. Zhu, *PhD Thesis*, University of Helsinki (Helsinki) **2015**.
- [181] G. Kalamani, D. Cheneler, L. M. Grover, M. J. Adams, J. Bowen, *J. Mech. Behav. Biomed. Mater.* **2014**, 36, 135.
- [182] D. Lee, H. Zhang, S. Ryu, *Elastic Modulus Measurement of Hydrogels*, Springer, Cham **2018**, pp. 1–21.
- [183] D. Mistry, H. F. Gleeson, *J. Polym. Sci. B: Polym. Phys.* **2019**, 57, 1367.
- [184] T. Xu, J. H. Yoo, S. Babu, S. Roy, J.-B. Lee, H. Lu, *J. Micromechan. Microeng.* **2016**, 26, 10.
- [185] W. Chen, C. Wang, L. Yan, L. Huang, X. Zhu, B. Chen, H. J. Sant, X. Niu, G. Zhu, K. N. Yu, V. A. Roy, B. K. Gale, X. Chen, *J. Mater. Chem. B* **2014**, 2, 1699.
- [186] G. Stamoulis, C. Wagner-Kocher, M. Renner, *J. Mater. Sci.* **2007**, 42, 4441.
- [187] K. Comley, N. A. Fleck, *Int. J. Solids Struct.* **2010**, 47, 2982.
- [188] M. Pawlaczyk, M. Lelonkiewicz, M. Wieczorowski, *Postepy Dermatol. Alergol.* **2013**, 30, 302.
- [189] B. C. W. Kot, Z. J. Zhang, A. W. C. Lee, V. Y. F. Leung, S. N. Fu, *PLoS One* **2012**, 7, e44348.
- [190] J. Y. Rho, R. B. Ashman, C. H. Turner, *J. Biomechan.* **1993**, 26, 111.
- [191] G. Tomaiuolo, *Biomicrofluidics* **2014**, 8, 5.
- [192] C. I. Buchanan, R. L. Marsh, *J. Appl. Physiol.* **2001**, 90, 164.
- [193] T. Shen, E. Benet, S. L. Sridhar, J. Abadie, E. Piat, F. J. Vernerey, *Acta Biomater.* **2019**, 85, 253.
- [194] Z. Xiong, M. L. Zheng, X. Z. Dong, W. Q. Chen, F. Jin, Z. S. Zhao, X. M. Duan, *Soft Matter* **2011**, 7, 10353.
- [195] M. P. Kummer, J. J. Abbott, B. E. Kratochvil, R. Borer, A. Sengul, B. J. Nelson, *IEEE Trans. Robot.* **2010**, 26, 1006.
- [196] N. Dechev, J. K. Mills, W. L. Cleghorn, in *ASME Int. Mechanical Engineering Congress and Exposition*, ASME/EDC, Anaheim, CA **2004**, pp. 447–456.
- [197] C. Yamahata, D. Collard, B. Legrand, T. Takekawa, M. Kumemura, G. Hashiguchi, H. Fujita, *J. Microelectromech. Syst.* **2008**, 17, 623.
- [198] R. T. Rajendra Kumar, S. U. Hassan, O. Sardan Sukas, V. Eichhorn, F. Krohs, S. Fatikow, P. Boggild, *Nanotechnology* **2009**, 20, 39.
- [199] J. Flynt, *What is FDM 3D Printing*, 3dinsider, San Francisco, CL **2018**.
- [200] All3DP, *Stereolithography (SLA) 3D Printing – Simply Explained* **2019**.
- [201] P. L. Baldeck, P. Prabhakaran, C.-Y. Liu, M. Bouriau, L. Gredy, O. Stephan, T. Vergote, H. Chaumeil, J.-P. Malval, Y.-H. Lee, C.-L. Lin, C.-T. Lin, Y. H. Hsueh, T.-T. Chung, *Optical Processes in Organic Materials and Nanostructures II*, Vol. 8827, SPIE, Bellingham, WA **2013**.
- [202] N. Fu, Y. Liu, X. Ma, Z. Chen, *J. Microelectron. Manuf.* **2019**, 2, 1.
- [203] C. Peters, M. Hoop, S. Pané, B. J. Nelson, C. Hierold, *Adv. Mater.* **2016**, 28, 533.
- [204] X. Wang, X. H. Qin, C. Hu, A. Terzopoulou, X. Z. Chen, T. Y. Huang, K. Maniura-Weber, S. Pané, B. J. Nelson, *Adv. Funct. Mater.* **2018**, 28, 1804107.
- [205] M. Dong, X. Wang, X. Z. Chen, F. Mushtaq, S. Deng, C. Zhu, H. Torlakcik, A. Terzopoulou, X. H. Qin, X. Xiao, J. Puigmartí-Luis, H. Choi, A. P. Pêgo, Q. D. Shen, B. J. Nelson, S. Pané, *Adv. Funct. Mater.* **2020**, 30, 17.
- [206] L. D. Zarzar, P. Kim, M. Kolle, C. J. Brinker, J. Aizenberg, B. Kaehr, *Angew. Chem.* **2011**, 123, 9528.



Georges Adam obtained his B.S. degree in mechanical engineering and engineering physics from Rose-Hulman Institute of Technology in 2017. He is currently pursuing his Ph.D. degree in mechanical engineering at Purdue University, West Lafayette, IN (USA) at the Multi-Scale Robotics and Automation Lab. His research interests include smart microrobotics and micromanipulation systems for biomedical applications, actuation, and sensing.



Amine Benouhiba graduated from the Preparatory School of Science and Technology, Algeria, in 2012. He received his engineering degree in material engineering from Ecole Nationale Polytechnique (ENP), Algeria, in 2015. He also received his master's degree in innovative materials from Ecole centrale de Lyon (ECL) in 2016. He completed his Ph.D. degree in 2020 at the Bourgogne-Franche-Comté University. Currently, he is a postdoctoral researcher at the same university. His research interests include the design and development of origami-inspired structures, microrobotics, and soft robotics.



Kanty Rabenoroso received the M.S. degree in electrical engineering from INSA Strasbourg, France, in 2007, and the Ph.D. degree in automatic control from the University of Franche-Comté, Besançon, France, in 2010. He was a postdoctoral fellow at LIRMM, University of Montpellier, France, from 2011 to 2012. He is currently an associate professor with the AS2M Department, FEMTO-ST Institute, Besançon. His research interests include mechatronics, smart actuator, and soft and continuum microrobotics at small scales for medical applications within the Micro-NanoRobotics team. He has participated in several European projects and ANR projects.



Cédric Clévy received his Ph.D. degree in automatic control and computer sciences in 2005 from the University of Franche-Comté, France. Since 2006, he has been an associate professor at the University of Bourgogne Franche-Comté, Besançon, France, working in the AS2M (Automatic Control and MicroMechatronic Systems) Department of FEMTO-ST Institute. His research interests are the design, modeling, and control of micro- and nanorobotic systems for the characterization, manipulation, and assembly at micro- and nanoscales.



David J. Cappelleri is an associate professor in the School of Mechanical Engineering at Purdue University. He received his B.S. degree from Villanova University, M.S. degree from The Pennsylvania State University, and Ph.D. degree from the University of Pennsylvania in mechanical engineering. His research interests include mobile microrobotics for biomedical and manufacturing applications, surgical robotics, automated manipulation and assembly, and unmanned aerial and ground robot design for industrial and agricultural applications.